

# ERA

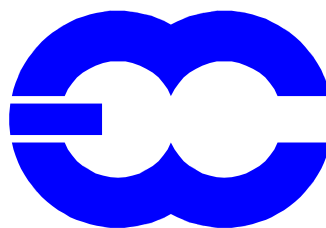
## ECMWF Re-Analysis Project Report Series

---

### 1. ERA-15 Description (Version 2 - January 1999)

J. K. Gibson, P. Kållberg, S. Uppala,  
A. Hernandez, A. Nomura, E. Serrano

European Centre for  
Medium-Range Weather  
Forecasts



Europäisches Zentrum für  
mittelfristige  
Wettervorhersage

Centre européen pour les prévisions météorologique à moyen terme



## ACKNOWLEDGEMENT

The ECMWF Re-Analysis (ERA) project would not have been possible without the active support and co-operation of many agencies, bodies, and individuals.

In addition to the Council of the European Centre for Medium-range Weather Forecasts, practical support in terms of finance, staffing, and/or the supply of data has been received from the following:

- University of California Lawrence Livermore National Laboratory
- The European Union
- Japan Meteorological Agency
- World Meteorological Organisation and World Climate Research Programme
- National Center for Atmospheric Research, Boulder, Colorado
- Cray Research Incorporated
- National Oceanic and Atmospheric Administration, National Centers for Environmental Prediction, Washington
- United Kingdom Meteorological Office
- Center for Ocean, Land, and Atmosphere Studies, Maryland, USA.
- National Snow and Ice Data Center, University of Colorado
- National Meteorological Centre, Melbourne

Permission to use data supplied is gratefully acknowledged.

ERA production data have been subjected to validation through specially commissioned validation projects. The advice and information provided by the ERA Validation Partners is gratefully acknowledged. Validation Partners included:

- Max-Planck-Institut für Meteorologie, Hamburg, Germany
- Direction de la Météorologie Nationale, France
- Koninklijk Nederlands Meteorologisch Instituut
- Istituto per lo Studio della Metodologie, IMGMA, Modena, Italy
- United Kingdom Meteorological Office
- University of Bologna, Italy
- Danish Meteorological Institute

The ERA project received advice from its External Advisory Group, whose members included:

Dr. J-C André, Météo France; Prof. Dr. Lennart Berntsson, Max-Planck-Institut; Dr. D. Blaskovich, Cray Research Incorporated; Dr. G. Boer, AES Canada; Dr. D. Carson, Hadley Centre, U.K.; Prof. W. L. Gates, PCMDI, University of California; Prof. B. Hoskins, University of Reading, U.K.; R. Jenne, NCAR; Dr. E. Kalnay, NMC Washington; Dr. R. Newson, WCRP, WMO; Dr. B. Orfila, European Climate Systems Network; Prof. J. Shukla, University of Maryland; Dr. C. Schuurmans, KNMI; Dr. O. Talagrand, LMD, Paris; Prof. S. Tibaldi, Bologna University; Dr. K. Trenberth, NCAR; Dr. W. Wergen, DWD.

The help and assistance given by ECMWF Staff, the other re-analysis groups throughout the world, and the many other interested parties too numerous to mention by name are gratefully appreciated

# ECMWF Re-Analysis Project Report Series

## 1. ERA-15 Description (Version 2 - May 1999)

### Contents

|                                                                  |    |
|------------------------------------------------------------------|----|
| 1. Introduction .....                                            | 3  |
| 2. Planning .....                                                | 4  |
| 2.1 Data Assimilation at ECMWF.....                              | 4  |
| 2.2 Initial considerations .....                                 | 5  |
| 2.3 Work programme.....                                          | 5  |
| 3. Input Data for the ECMWF Re-Analysis .....                    | 7  |
| 3.1 Data sources.....                                            | 7  |
| Satellite radiance data .....                                    | 7  |
| Cloud track winds .....                                          | 9  |
| Other observations .....                                         | 10 |
| 3.2 Data sources - forcing fields.....                           | 11 |
| 3.3 Acquisition and preparation of data .....                    | 12 |
| Pre-processing of the CCR data.....                              | 12 |
| Pre-processing of NESDIS 1-b data .....                          | 13 |
| Pre-processing of other observations .....                       | 13 |
| Preparation of the forcing fields .....                          | 14 |
| 3.4 Conformity with other re-analysis projects .....             | 14 |
| 4. Experimentation .....                                         | 15 |
| 4.1 Vertical Resolution.....                                     | 15 |
| 4.2 Timeliness of first guess with respect to observations ..... | 17 |
| 4.3 Orography .....                                              | 17 |
| 4.4 Soil.....                                                    | 18 |
| 4.5 Clouds.....                                                  | 18 |
| 5. The ECMWF Re-Analysis Data Assimilation Scheme. 21            |    |
| 5.1 One dimensional variational analysis (1D-Var) .....          | 22 |
| The 1D-Var method .....                                          | 22 |
| Bias corrections for 1D-Var.....                                 | 22 |
| The use of retrievals in the analysis .....                      | 23 |
| 5.2 The analysis .....                                           | 23 |
| Monitoring, bias correction, and observation blacklists .....    | 24 |

|                                                    |    |
|----------------------------------------------------|----|
| The analysis and quality control.....              | 26 |
| The assumed observation errors .....               | 26 |
| The assumed “First Guess” (FG) errors .....        | 27 |
| Objective optimum interpolation analysis.....      | 27 |
| Snow cover .....                                   | 28 |
| Soil Moisture .....                                | 28 |
| The normal mode initialisation.....                | 28 |
| 5.3 The ECMWF global atmospheric model .....       | 29 |
| The model formulation .....                        | 29 |
| The basic equations .....                          | 29 |
| The resolution in time and space .....             | 30 |
| The numerical formulation .....                    | 32 |
| Parametrization of physical processes.....         | 33 |
| 6. Production .....                                | 40 |
| 6.1 Overview .....                                 | 40 |
| 6.2 Production system design.....                  | 41 |
| 6.3 Organising the observations.....               | 42 |
| 6.4 Data assimilation .....                        | 43 |
| 6.5 Adding results to the archive.....             | 45 |
| 6.6 Checking the archive files .....               | 46 |
| 6.7 Production log .....                           | 46 |
| 6.8 Post-production log .....                      | 48 |
| 7. Re-Analysis Output.....                         | 51 |
| 7.1 Analysis and Forecast Fields.....              | 51 |
| Daily data.....                                    | 51 |
| Monthly data.....                                  | 55 |
| 7.2 Data from ERA - observations and feedback..... | 61 |
| 7.3 Other data .....                               | 61 |
| 7.4 Availability of ERA data.....                  | 61 |
| 8. Concluding Remarks .....                        | 62 |
| References:.....                                   | 63 |
| Bibliography:.....                                 | 67 |

# ECMWF Re-Analysis Project Report Series

## 1. ERA-15 Description (Version 2 - May 1999)

### List of Tables

|                                                                                                         |    |
|---------------------------------------------------------------------------------------------------------|----|
| Table 1 - Cloud cleared radiance data were used from the following satellites for the periods indicated | 8  |
| Table 2 - Periods when ECMWF retrievals from NESDIS I-b data were used to supplement gaps in CCR data.  | 9  |
| Table 3 - Sea Surface Temperature used by the ECMWF Re-Analysis                                         | 12 |
| Table 4 - Pressure of model levels when the surface pressure is 1015 hPa                                | 31 |
| Table 5 - Events from the Production Log.                                                               | 47 |
| Table 6 - Upper Air Parameters - daily archive                                                          | 52 |
| Table 7 - Surface and single level parameters - daily archive                                           | 53 |
| Table 8 - Upper Air Parameters - monthly means and monthly “daily” means                                | 55 |
| Table 9 - Upper Air Parameters - variance and co-variance dats                                          | 56 |
| Table 10 - Surface and single level parameters - monthly archive                                        | 58 |
| Table 11 - Forecast accumulations - monthly mean data                                                   | 60 |





# ECMWF Re-Analysis Project Report Series

## 1. ERA-15 Description (Version 2 - May 1999)

### List of Figures

|         |                                                                                                                                                                                                                            |
|---------|----------------------------------------------------------------------------------------------------------------------------------------------------------------------------------------------------------------------------|
| Page 4  | Figure 1 - Data assimilation using 6 hour cycles                                                                                                                                                                           |
| Page 8  | Figure 2 - Availability and use of cloud cleared radiance data.                                                                                                                                                            |
| Page 16 | Figure 3 - Root mean square fit of radiosonde meridional winds to the first guess, 20°N to 20°S, for three weeks in January 1993. Full line 19 levels, dashed line 31 levels                                               |
| Page 16 | Figure 4 - Root mean square fit of Northern Hemisphere (North of 20°N) temperatures to the analyses, for three weeks in January 1993. Full line 19 levels, dashed line 31 levels                                           |
| Page 19 | Figure 5 - Difference, in octas, between the annual mean total cloud cover from the prognostic and diagnostic cloud schemes. Blue colours indicate more clouds in the prognostic (ERA) scheme                              |
| Page 20 | Figure 6 - Difference in W/m <sup>2</sup> between the annual mean surface net energy fluxes from the prognostic and diagnostic cloud schemes. Positive values indicate LESS energy loss from the surface to the atmosphere |
| Page 24 | Figure 7 - The use of TOVS retrievals in the ERA analyses                                                                                                                                                                  |
| Page 25 | Figure 8 - Difference information contained in “analysis feedback”.                                                                                                                                                        |
| Page 30 | Figure 9 - The 31-level vertical resolution                                                                                                                                                                                |
| Page 42 | Figure 10 - principal concentrations of data associated with the main processing components of ERA.                                                                                                                        |
| Page 44 | Figure 11 - The main components of the ERA system.                                                                                                                                                                         |





---

*ERA-15  
Description  
(Version 2 - May  
1999)*

---



# ECMWF Re-Analysis Project Report Series

## 1. ERA-15 Description (Version 2 - May 1999)

J. K. Gibson, P. Kållberg, S. Uppala, A. Hernandez, A. Nomura, E. Serrano

### 1. Introduction

ECMWF began its operational activities in 1979. Since then the Centre's archive of analyses and forecasts has become an important source of data for research. It is used extensively by the Centre's staff and by scientists from all over the world for a wide variety of studies and applications. In recent years this archive has been the basis for the ECMWF TOGA (Tropical Ocean Global Atmosphere) data set, providing analyses of the global atmosphere for TOGA research.

Operational analyses, while providing a valuable resource for research, are affected by the major changes in models, analysis technique, assimilation, and observation usage which are an essential product of research and progress in an operational numerical weather prediction centre. They also can make use only of those observations which become available within near real time. Many years ago Bengtsson and Shukla (1988) expressed the idea that such considerations provide valid reasons for performing a consistent re-analysis of atmospheric data. Typical research applications which could make good use of re-analyses include studies of predictability, observing system performance, general circulation diagnostics, atmospheric low-frequency variability, the global hydrological and energy cycle and coupled ocean-atmosphere modelling.

The first ECMWF Re-Analysis (ERA) project has produced a new, validated 15 year data set of assimilated data for the period 1979 to 1993 (ERA-15). The project began in February 1993. The first phase of the work required the acquisition and preparation of the observations and forcing fields. During the first year a substantial programme of experimentation, closely co-ordinated with the Centre's Research and Operational activities was completed. This enabled the scientific components of the re-analysis system to be defined, and a strategy for production to be determined. At the same time work was progressing on the development of both the production system and the internal validation tools. The final production system was adopted in 1994, and there followed a period of sustained production, monitoring and validation throughout 1995 and the first nine months of 1996.

All data generated by the project likely to be of future value have been collected and preserved. These include blacklist information, radiosonde bias correction tables, TOVS bias and calibration files, and the record of which satellites have been used at different periods.

## 2. Planning

### 2.1 Data Assimilation at ECMWF

In many areas of the globe the density of available observations is far below that needed to support the analysis with the required accuracy. In such areas a simple analysis would rely mainly on satellite based observations: cloud cleared radiance data or retrieved temperature and humidity data from the NOAA satellites, and cloud motion wind data from geostationary satellites.

A data assimilation scheme attempts to make use of a numerical forecast model to propagate information concerning the state of the global atmosphere from data rich areas to data sparse areas. Output from the forecast model is used, together with the observations and forcing fields, as input to the analysis. Results from the analysis, after initialisation, are then used as initial conditions for the next forecast. These processes are repeated in a cyclic fashion, as illustrated in Figure 1.

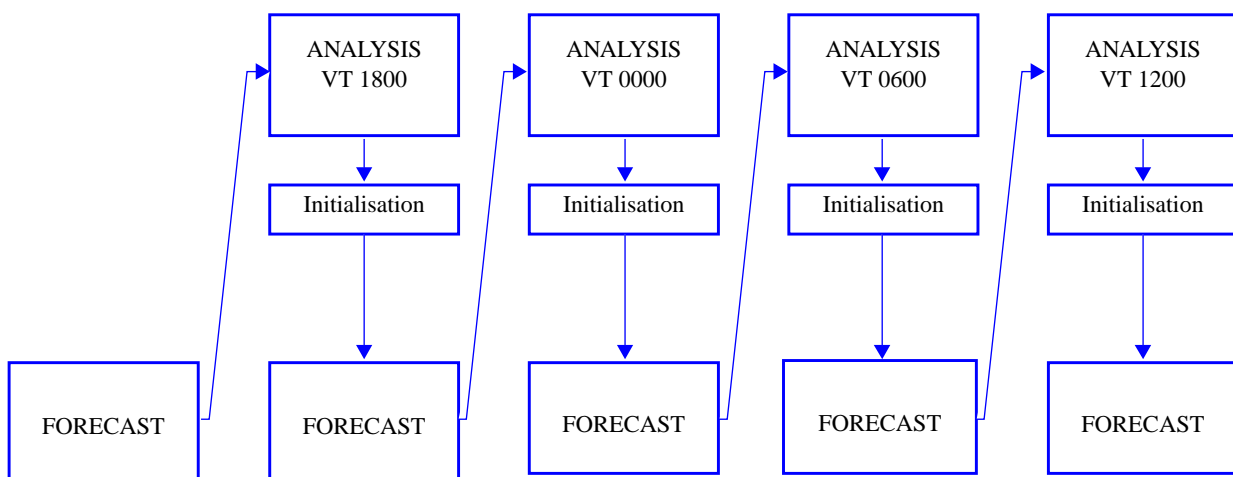


Figure 1- Data assimilation using 6 hour cycles

Thus, continuous data assimilation over a long period is really equivalent to running the forecast model as a global circulation model and relaxing towards the observations and forcing fields at six hourly intervals.

## 2.2 Initial considerations

If a data assimilation scheme of the type outlined above is to be used for re-analysis over a given period, the following must be considered in some detail before the actual production work can be attempted:

- the observations and forcing fields to be used as input;
- the acquisition, preparation, and checking required with respect to these input data
- the exact composition of the assimilation system to be used;
- what data the production system should generate;
- how the production should be monitored and validated;
- what data should be archived;
- how end users can be given access to the data;
- what other deliverables, such as documentation and reports, the project should be required to deliver.

To enable this to be done two advisory bodies were set up - an internal steering group, and an external advisory board.

The external advisory group provided contact with the potential end-users of the re-analyses, and was of particular assistance in helping to determine the archive policy. Members of this group also provided valuable opinion with respect to many of the scientific choices which had to be made.

The internal steering group provided critical input to the initial planning, the decision making with respect to the production system components, and the archive policy. Steering group meetings also provided the essential discussion and exchange of information without which the excellent level of co-operation enjoyed between the project staff and other groups within ECMWF would not have been possible.

## 2.3 Work programme

Early planning effort resulted in a work programme which required a number of objectives to be achieved.

It was decided to acquire a number of additions to the archive of observations accumulated from ECMWF's daily operations. The acquisition and preparation of these additional data would need to have been completed for any particular year before re-analysis of that year could take place.

It was also necessary to acquire appropriate forcing fields in the form of sea surface temperatures (SST), and sea-ice cover. The various candidate data sets would then need to be examined carefully so that a decision could be made on which to use.

The re-analysis production was to be carried out with an invariant data assimilation system. There were a number of decisions which needed to be made with regard to the exact configuration of the analysis system, and also of the forecast model. The resolution to be used both in the vertical and the horizontal would need to be decided. Thus it was considered necessary to embark on a number of controlled experiments to assess the various available options.

A production system capable of sustaining the required rate of re-analysis had to be designed and assembled. It would need to include sufficient monitoring components to enable problems to be intercepted, and reasonable confidence to be established with respect to the on-going generation of results. The system needed to be checked out carefully to ensure that it performed correctly from both a scientific and technical point of view. Optimization would be necessary to achieve the required production rate.

A validation programme, including the setting up of a number of external validation projects was envisaged to ensure that the re-analysis results achieved the goal of the production of a validated set of data. The following entered into contracts as external validation partners:

Max Plank Institut für Meteorologie, Hamburg, Germany (MPI);

Hadley Centre, Meteorological Office, Bracknell, U.K. (UKMO);

Météo-France, Toulouse, France (DMN);

Danish Meteorological Institute, Copenhagen, Denmark (DMI);

Royal Netherlands Meteorological Institute, De Bilt, Netherlands (KNMI);

Instituto per lo studio delle Metodologie Geofisiche Ambientali, CNR, Modena, Italy (IMGA);

Atmospheric Dynamics Group, University of Bologna Italy (ADGB).

During production it would thus be necessary to make results and information concerning progress available to the validation teams. The precise data to be generated to form the results of the re-analysis had to be specified, and the archive designed. As much archive construction as possible would need to be accomplished during the production, so as to minimise the residual tidy-up work necessary at the end of production.

To complete the project it would be highly desirable to produce a good set of documentation, and to organise the observations, the forcing fields, and the information gained during the production in such a way that it would be of maximum benefit to any future re-analysis.



### 3. Input Data for the ECMWF Re-Analysis

The data used for the re-analysis, their acquisition, and the work done to prepare them for the assimilation system are described in this section.

#### 3.1 Data sources

The ECMWF Archive contains all observational data acquired in real time from the World Meteorological Organisation's Global Telecommunications System (GTS) since the beginning of daily operations in 1979. An archive of First GARP Global Experiment (FGGE) level II-b data was also on-site at ECMWF. To provide a comprehensive set of input data for ERA data were acquired from a number of additional sources.

##### 3.1.1 Satellite radiance data

The 250 km cloud cleared radiance (CCR) data were acquired from the World Data Centre at Ashville. These data contains layer-mean virtual temperature for 15 standard layers, layer precipitable water content for 3 layers, cloud cleared brightness temperatures and various identification parameters.

The TIROS Operational Vertical Sounder (TOVS) measures multi-spectral radiances, which are related to the temperature and humidity structure in the atmosphere. Since 1979 the National Environmental Satellite Data Information Service (NESDIS) have routinely produced CCR data. The method followed is: first the completely cloud free fields of view (spots) are identified and selected; next those spots which are partly clear are processed to extract the radiances for the clear areas from the cloud-contaminated radiances; for the remaining spots only microwave radiances can be used. The radiances after cloud clearing are thus identified as clear, partly cloudy or cloudy. Until 10 June 1980 cloud clearing was done with the algorithm described by Smith and Woolf (1976); for later data NESDIS used the method of McMillin and Dean (1982).

The quality of satellite retrievals varies considerably over the years. The causes of this variability are mainly related to the processing of the raw data. Generally the same instruments, High-resolution Infra-red Radiation Sounder (HIRS), Microwave Sounding Unit (MSU), and Stratospheric Sounding Unit (SSU) were used with the same specifications on all satellites. There are some minor exceptions, notably with respect to the channel 10 centre frequency for the HIRS unit on NOAA-11, but these are thought to have had little impact on the assimilations. Figure 2 illustrates the availability of data from the various NOAA satellites throughout the ERA period.

The cloud cleared radiance archive provided an almost continuous source throughout the ERA period. Unfortunately, however, there were a number of periods for which the archive was not complete. Where gaps occurred for only a few analysis cycles production was allowed to continue without the use of cloud cleared

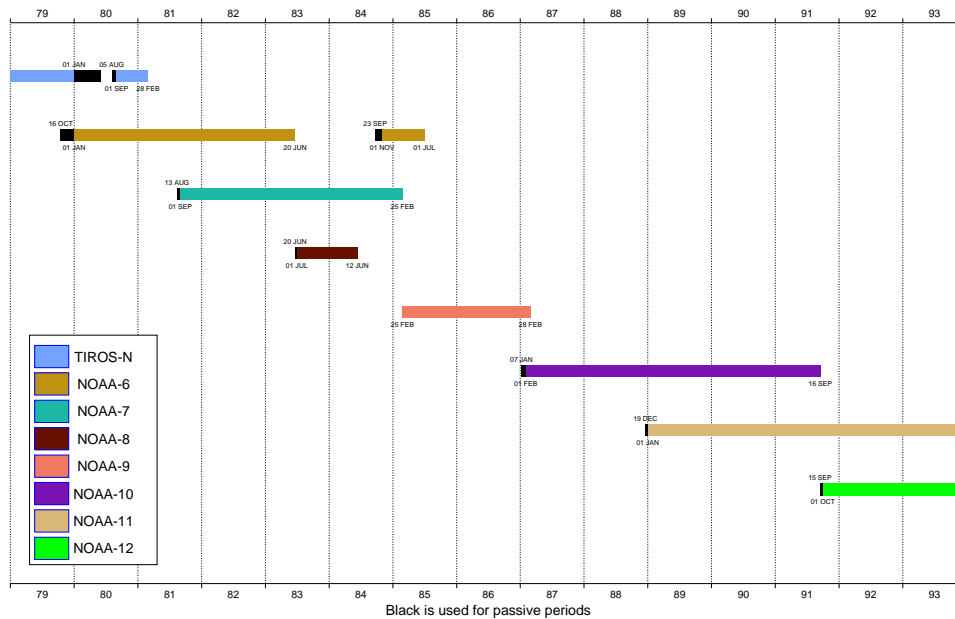


Figure 2 - Availability and use of cloud cleared radiance data.

radiance data. Table 1 on page 8 provides information concerning which satellites were used for which periods. Where longer gaps occurred steps were taken to generate ECMWF retrievals from level 1b raw radiance data. Table 2 on page 9 lists the periods for which ECMWF retrievals produced from NESDIS 1b data were used to supplement such gaps

**Table 1 - Cloud cleared radiance data were used from the following satellites for the periods indicated**

| PERIOD                   | SATELLITES USED   | COMMENTS                                       |
|--------------------------|-------------------|------------------------------------------------|
| 01.12.1978 to 31.12.1978 | None              | TIROS-N only became operational January 1979   |
| 01.01.1979 to 31.12.1979 | TIROS-N only      |                                                |
| 01.01.1980 to 31.05.1980 | NOAA-6 only       | Data from MSU3 not used                        |
| 01.06.1980 to 31.08.1981 | NOAA-6 only       |                                                |
| 01.09.1981 to 20.06.1983 | NOAA-6 and NOAA-7 | NOAA-6 not used June 1983                      |
| 21.06.1983 to 12.06.1984 | NOAA-7 and NOAA-8 | NOAA-8 not used June 1983                      |
| 13.06.1984 to 31.10.1984 | NOAA-7 only       | Data from some channels not available at times |

**Table 1 - Cloud cleared radiance data were used from the following satellites for the periods indicated**

|                          |                     |                                                |
|--------------------------|---------------------|------------------------------------------------|
| 01.11.1984 to 31.01.1985 | NOAA-6 and NOAA-7   | Data from some channels not available at times |
| 01.02.1985 to 31.03.1985 | NOAA-6 only         | Data from some channels not available at times |
| 01.04.1985 to 06.01 1987 | NOAA-9 only         |                                                |
| 07.01.1987 to 31.03.1989 | NOAA-10 only        |                                                |
| 01.04.1989 to 30.09.1991 | NOAA-10 and NOAA-11 |                                                |
| 01.10.1991 to 28.02.1994 | NOAA-11 and NOAA-12 |                                                |

**Table 2 - Periods when ECMWF retrievals from NESDIS I-b data were used to supplement gaps in CCR data.**

|                      |                      |                      |
|----------------------|----------------------|----------------------|
| 02.10.83 to 04.10.83 | 01.07.87 to 19.07.87 | 29.01.89 to 02.02.89 |
| 13.04.86 to 01.07.86 | 26.07.87 to 29.07.87 | 03.09.90 to 12.09.90 |
| 28.07.86 to 05.08.86 | 23.08.87 to 30.08.87 | 01.02.91 to 06.02.91 |
| 11.09.86 to 13.09.86 | 08.01.89 to 18.01.89 |                      |

### 3.1.2 Cloud track winds

Cloud track winds (SATOB) data were specially generated for inclusion within the First GARP Global Experiment (FGGE) level II-b data set. As part of the special effort for FGGE a GOES satellite was positioned over the Indian Ocean. After the end of FGGE (November 1979) SATOB data were gradually introduced into the real-time data distribution service of the WMO GTS. However the amounts of SATOB data dropped dramatically after FGGE; Meteosat SATOB winds were not produced operationally until August 1982, and there are no reliable SATOB winds from the Indian Ocean from December 1979 onwards.

JMA generously made available a complete copy of the archive of cloud track winds from the GMS satellite.

SATOB data were used in the re-analysis between 50N-50S. For each satellite, data were used only within specific longitude limits, as follows:

- METEOSAT 50W-50E
- GOES 160W-60W

- HIMAWARI 90E-170W

In addition the following restrictions were applied:

- METEOSAT:
  - Not used over land between 50N and 35N.
  - Not used over land between 35N and 20N when  $P > 500$  hPa.
  - Not used over land between 20S and 50S when  $P > 500$  hPa.
- GOES:
  - Not used between 50N and 20N when  $P < 700$  hPa.
  - Not used over land between 50N and 20N.
  - Not used over land between 20S and 50S when  $P > 500$  hPa.
- HIMAWARI:
  - Not used between 50N and 20N when  $P < 700$  hPa.
  - Not used over land between 50N and 20N.
  - Not used over land between 20S and 50S when  $P > 500$  hPa.
  - Not used between 20S and 50S when  $P < 700$  hPa.
- INSAT:
  - not used.

### 3.1.3 Other observations

The principal source of conventional observations has been the ECMWF real-time data collection from the Meteorological Archive and Retrieval System (MARS). These data are acquired from two major nodes on the World Meteorological Organisation's Global Telecommunications Network (WMO GTS). Little, if any data are distributed within the GTS with a cut-off of more than 24 hours. Nevertheless up to three days accumulation of data is allowed at ECMWF before they are added to the archive. ECMWF daily operations began in 1979; in consequence it can be expected that these data may not be as complete for the early months as for the majority of the period of interest. It should be noted that although the most important observational data are exchanged globally via the GTS, there are differences with respect to regional and national data in the availability of data from any one node.

For 1979 the principal source of observations was the First GARP Global Experiment (FGGE) level II-b data set. During FGGE a considerable number of special observations were made, particularly in the tropics. There was also an immense effort during FGGE to collect all observations made. In December 1979, after the

FGGE year, the number of radiosonde observations dropped significantly. In 1980, the first full year of ECMWF operations, not all potentially available observations were being acquired. From 1981 the radiosonde coverage increased, but was still below that potentially available. PILOT data amounts are fairly constant during the period; in 1980 they are almost the only upper air data source (except CCR) over the Indian Ocean.

Ship and buoy observations were augmented by adding data from the Comprehensive Ocean Atmosphere Data Set (COADS) (Woodruff et al., 1993). Additionally, buoy data from the TOGA and SUBDUCTION experiments were obtained.

The level II-b data from the Alpine Experiment were acquired from the University of Innsbrück. Data from most other observing experiments were found to have been distributed via the GTS.

The Japan Meteorological Agency (JMA) archive was found to contain considerably more aircraft data over the North Pacific than the MARS archive; it also included more radiosonde data from the immediate area around Japan. These differences are likely to be due to the regional and national practices applied at different GTS nodes. Appropriate sub-sets of this archive were kindly supplied by JMA to help rectify these deficiencies.

Operational experience at ECMWF had established the importance of making use of the surface pressures from the pseudo observations called “PAOBS” generated by the National Meteorological Centre at Melbourne. The Australian Bureau of Meteorology kindly made available a copy of their PAOB archive.

It had been hoped to include dropsonde data for the TOGA COARE period, and also from the BASE experiment. These data were acquired, but technical difficulties associated with their use within the ERA assimilation system prevented their inclusion.

### **3.2 Data sources - forcing fields**

The externally prescribed forcing of the re-analyses, in addition to the observations, comes from the sea surface temperatures (SST) and the sea ice cover.

Sea ice cover, though potentially available from the sea surface temperature data sets, was derived separately at ECMWF from SMMR and SSM/I data, using a scheme devised as part of the ERA project (Nomura, 1997).

For most of the re-analysis (November 1981 to February 1994) sea surface temperatures from the National Centers for Environmental Prediction (NCEP) in Washington (Reynolds, 1994) were obtained. These are at a

1 degree resolution, and are available weekly. They were generated using an optimal interpolation technique, and make use of satellite and in-situ data.

For the period before November 1981 the Meteorological Office 1 degree monthly Global sea-Ice and Sea Surface Temperatures (GISST) version 1.1 (Parker et al., 1995) were acquired initially. However, at a later date it was decided to re-run the whole of 1979 and part of 1980. It was also considered highly desirable to use the same observations and forcing fields as the NCEP re-analysis for 1979. At the time of the re-run, GISST version 2.2 (Rayner et al., 1996) was available and had been used by NCEP. The 1979 GISST sea surface temperatures were thus acquired and used, while the re-run of 1980 made use of the original GISST 1.1 data. Table 3 illustrates the use of sea surface temperature data throughout the re-analysis

**Table 3 - Sea Surface Temperature used by the ECMWF Re-Analysis**

| Period                | SST Data Used                  | Reference           |
|-----------------------|--------------------------------|---------------------|
| December 1978         | GISST version 1.1<br>(monthly) | Parker et al., 1995 |
| 1979                  | GISST version 2.2<br>(monthly) | Rayner et al., 1996 |
| 1980 to October 1981  | GISST version 1.1<br>(monthly) | Parker et al., 1995 |
| November 1981 onwards | NCEP OI (weekly)               | Reynolds, 1994      |

### 3.3 Acquisition and preparation of data

ECMWF have adopted the WMO standards for binary data representation. All additional input data for ERA were first converted to the WMO code forms FM92 GRIB (for fields) or FM94 BUFR (for observations).

#### 3.3.1 Pre-processing of the CCR data

The CCR Data were received from NCAR on IBM 3480 tape cartridges. These were read, converted into BUFR, then stored until required. For each satellite a monthly time series of the mean six hour brightness temperatures for each channel was plotted together with the corresponding number of data. This provided information relating to periods of channel deficiencies, and contributed towards the identification of which satellite(s) could best be used for which periods. A NOAA/NESDIS document (NESDIS, 1993) provided a list of the most important changes or errors (e.g. mis-location of data) as well as changes in the software used to calculate the CCR data. Most of these events are difficult to identify from brightness temperatures alone, since their effects are relatively small.

Occasionally there were miss-located soundings in the CCR data-set, especially during the first few days of a year. As part of the quality control, the latitude and longitude of the soundings were checked and the wrong locations corrected, using a set of orbital elements provided by NESDIS, and a diary of earth-location problems was made.

### **3.3.2 Pre-processing of NESDIS 1-b data**

A number of gaps were identified with respect to the 250 km cloud cleared radiance data; a system was prepared, with the aid of the Satellite Data Section, to fill these gaps using the NESDIS I-b data.

First, orbits without either MSU or HIRS measurements were rejected, duplicated data eliminated, and the files re-structured in a form convenient for further processing. These files were then stored until required by the production suite.

During the production, 1-b data were pre-processed, ingested, and cloud cleared. The software to accomplish this was adapted for use in the ERA system from the International TOVS Processing Package (ITPP4). The cloud clearing module used the first guess forecast of the surface temperature in the tests for detection of clear fields of view.

### **3.3.3 Pre-processing of other observations**

Observations from MARS were extracted for periods well ahead of the ERA production. They were then passed through a conversion programme to ensure that they could be read, and to convert old editions of BUFR to the current edition. The converted data were categorized into conventional data, ships, buoys, and satellite data. The ships and buoys were further categorized into those containing non-trivial identifiers and those annotated simply "SHIP". Resulting files were stored until required.

FGGE and ALPEX data were first converted from the FGGE II-b format to BUFR, then organized into files and stored until required.

The additional observations received from JMA were converted into BUFR and stored. These data include additional TEMP and AIREP data from the North Pacific, and a full set of GMS cloud winds. The GMS cloud winds only became available after ERA production had reached 1981; they have been used from May 1981 onwards, and for the January to August 1980 re-run, but not for the period September 1980 to April 1981.

### 3.3.4 Preparation of the forcing fields

The SST data were interpolated from their original  $1^\circ \times 1^\circ$  resolution to the ERA Gaussian grid, and then linearly in time to the actual analysis time. There is no separate field in ERA describing the sea-ice distribution; instead it is defined as sea points with SST values below  $-1.8^\circ\text{C}$ . The sea-ice distribution is determined from SMMR and SSM/I data, available on CD-ROM (NSIDC, 1992; NSIDC, 1993). Since an ERA gridpoint is either land or sea, partial ice-cover is not possible. Sea areas where the SSMR-SSM/I data indicate more than 55% ice cover are defined as sea-ice, other points as open water (Nomura, 1997). The limit 55% was chosen based on comparisons between the satellite data and manual sea-ice analyses from operational centres. The sea-ice areas in the original SST analyses included partially ice covered areas and were found to be too large.

### 3.4 Conformity with other re-analysis projects

Since the National Centers for Environmental Prediction (NCEP), Washington, and NASA's Data Assimilation Office (DAO) are also producing re-analyses it was considered desirable to have at least one year during which each of the re-analysis projects would use the same input data. To this end a special effort was made to enable each of the three centres to use an identical set of observations, sea surface temperatures, and ice limits for 1979. ECMWF's contribution to this effort was to make available the FGGE observations in BUFR, and the sea-ice limits.



## 4. Experimentation

Before commencing the re-analysis, it was necessary to define the assimilation system to be used. Our goal was to use a modern but proven data assimilation, not necessarily identical to the system being used for the ECMWF operations at the time. Hence we selected ‘traditional’ optimum interpolation (OI) rather than the newer variational analysis, which was under development at the centre at the time and implemented operationally in 1996. Also, to conserve resources, it was pre-determined that the re-analyses should be accomplished with a horizontal spectral resolution of T106, corresponding to a Gaussian grid resolution of 1.125 degrees or about 125 km.

Based on in house experience and advice from both the external advisory group and the steering group, a set of parallel data assimilation and forecast experiments were carried out.

### 4.1 Vertical Resolution

The vertical resolution was examined in a three week experiment with two resolutions, 19 and 31 hybrid levels, with the increased resolution concentrated in the free troposphere and lower stratosphere in the 31-level version. The results showed that the fit of the first guess to the observations (OB-FG) was clearly better with the higher resolution for both horizontal wind components of the TEMP/PILOT reports. In the northern hemisphere (NH) this improvement was consistent from the mid-troposphere upwards, while in the tropics the improvement was concentrated between 300hPa and 70 hPa. Figure 3 shows the 31-level improvement in OB-FG for the meridional wind component between 20°N and 20°S. In the southern hemisphere (SH) the differences were small and inconclusive due to the small amount of data in relation to the number of TOVS profiles. Importantly, the improvement in the fit of the observed winds was retained through the initialisation.

The temperatures showed a similar behaviour, most pronounced around the tropopause where the 19-level resolution was inadequate. This is seen for example in the fit of the analysis to the observations (OB-AN), which depict how well the analysis is able to represent the TEMP soundings. In the Northern Hemisphere the OB-AN root mean square “misfit” of the analyses to the soundings is reduced from almost 1.5K to just about 1.0K between 250hPa and 300hPa (figure 4). Zonal averages of the meridional wind over the three weeks show that the 31 levels assimilation produced a 20% stronger Hadley cell outflow around 200hPa. The eddy kinetic energy was about 2% more lively in the higher resolution.

Two sets of 21 10-day forecasts were also run. The differences were in general small, although we noted a slight improvement in the NH 1000hPa scores from the higher resolution. In the SH the low resolution forecasts were the better, which is interesting since, in these early tests, the TOVS data were handled differently in the two hemispheres. In the NH radiances were used to produce physical retrievals with the

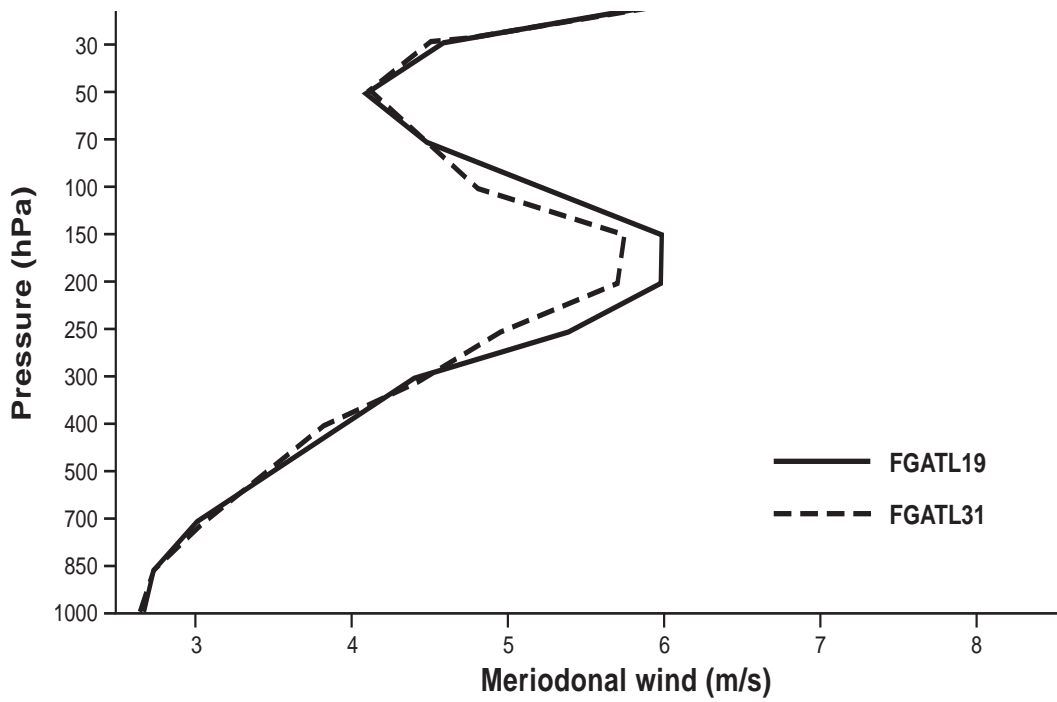


Figure 3 - Root mean square fit of radiosonde meridional winds to the first guess, 20°N to 20°S, for three weeks in January 1993. Full line 19 levels, dashed line 31 levels

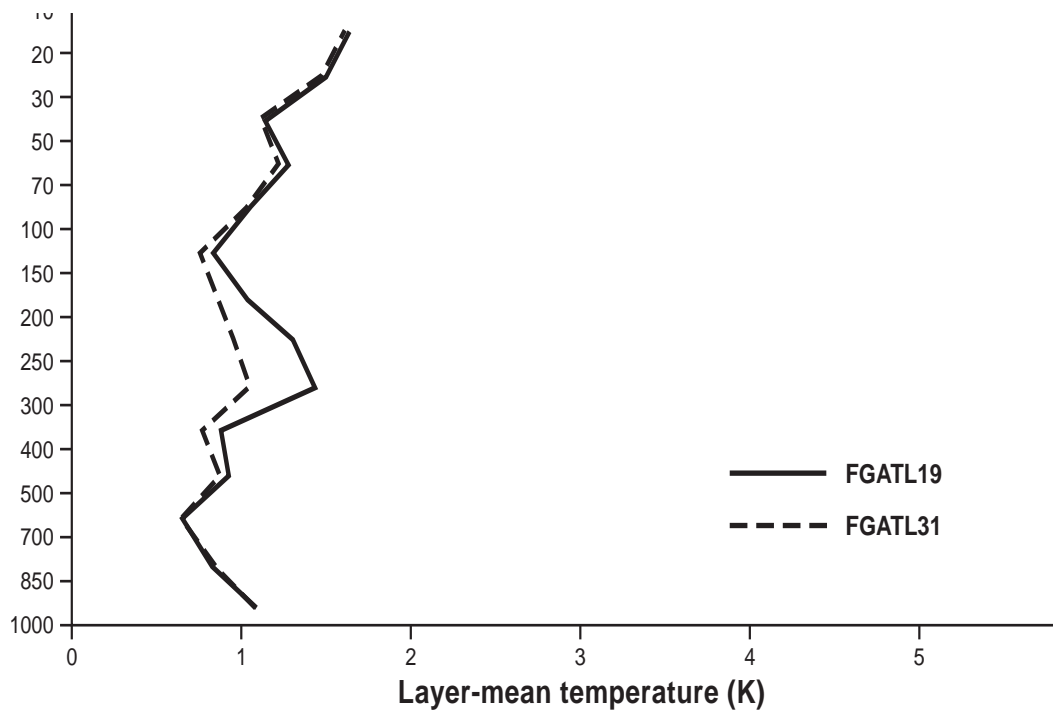


Figure 4 - Root mean square fit of Northern Hemisphere (North of 20°N) temperatures to the analyses, for three weeks in January 1993. Full line 19 levels, dashed line 31 levels

variational method (1D-Var), while in the SH the operational NESDIS retrievals were used. In the SH TOVS data dominate since there are few radiosondes, and it is evident that the NESDIS profiles do not benefit from the higher vertical model resolution. In the NH on the other hand the finer details added by the more abundant TEMP data were described better with the higher resolution. Such details are also subsequently retained better in the analysis through the variational use of the TOVS radiances.

## 4.2 Timeliness of first guess with respect to observations

The first O/I scheme introduced into ECMWF operations used 6 hour cycling, with a six hour forecast providing the first guess conditions. Later, a method called First Guess at Appropriate Time (FGAT) was introduced, and had been used for several years (Vasiljevic, 1990). In the FGAT approach the OB-FG increments are calculated from first guess information based on 3-hour, 6-hour, and 9-hour forecasts. These forecasts provided more timely first guess information with respect to the times of the observations, since the observations included data for a 6-hour period centred on the analysis time.

The FGAT scheme is considerably more expensive both in terms of computing time and file handling. A comparison with a NoFGAT assimilation was made in a three-week parallel analysis/forecast experiment. FGAT was seen to give a marginally positive impact in the OB-FG data fit, primarily in the MSL pressure near rapidly developing oceanic systems. These differences were however soon lost in the following forecasts, and we could not detect a significant impact in any of the 21 individual 10-day forecasts run as part of this experiment. In view of the considerable increase of the work load for FGAT, the NoFGAT method was selected for ERA.

## 4.3 Orography

Sub-gridscale orographic effects such as stagnant air in mountain valleys were for a long time parametrized at ECMWF by the use of an envelope orography, in which the gridpoint mean height was increased in proportion to the sub-gridscale variance in the US Navy 10' by 10' database used to define the orography. (Wallace et al., 1983). The envelope orography was however known to reduce the number of observations used in mountainous areas, and it also had some negative effects on the medium-range forecasts. In a three-week parallel experiment up to 10-15% more observations were accepted with mean orography at 1000hPa and 925hPa, both SYNOP and perhaps more importantly, TEMP. In another assimilation experiment a new parametrization of the effects of sub-gridscale orography which also includes a revised formulation of the gravity wave drag was tested successfully in the re-analysis configuration. See Lott and Miller (1997) for a description and evaluation of the formulation.

## 4.4 Soil

ECMWF had for many years used a two-level soil scheme with prescribed climatological temperature and moisture in the lower layer. The use of a prescribed soil climatology has the obvious risk of forcing a re-analysis towards its climate, which may be based on sparse information and may suffer from inconsistencies. Hence the new four level self-contained soil parametrization scheme developed by Viterbo and Beljaars (1995) for operational implementation was also selected for ERA and tested in a parallel assimilation experiment, which for reasons explained below is somewhat obsolete and will not be described here.

## 4.5 Clouds

After the experimentation described above and several other tests which were of a more technical or, in view of later developments obsolete, nature, the production began in earnest in December 1994, starting from 1979, the FGGE year. At this time the operational diagnostic cloud scheme (Slingo, 1987) had been selected for ERA use.

After a few months of the initial production had been run our monitoring indicated that a surface temperature warm bias, which was causing problems in the daily operations, was also apparent in the re-analyses. This was attributed to problems in the cloud cover, particularly over mid-latitude land areas in springtime, where unrealistic heating and drying was found to be due to too few clouds. As a quick remedy a very simple nudging scheme was introduced in which the soil moisture was adjusted towards the near-ground atmospheric humidity analyses (Viterbo, 1994, Viterbo, 1996, Mahfouf, 1991). Although the nudging reduced the bias problem, the more fundamental problem of too few clouds was still apparent.

Meanwhile a new cloud scheme with prognostic equations for cloud water content and cloud fraction, but without cloud advection, had approached maturity and had in tests been shown to yield more realistic clouds (Tiedtke, 1994 and Jakob, 1995). The re-analysis was stopped when production had reached the end of 1979 and another set of parallel assimilations was run for July 1985 and January 1986 with a thoroughly revised physics package. This, in addition to the prognostic cloud scheme and the soil moisture nudging, also contained revisions to the oceanic albedo for short wave radiation by Morcrette, and to the shallow convection by Nordeng. The results of these tests were so encouraging that it was decided to go back and restart the entire re-analysis from 1979 with the new physics.

The two complete 1979 assimilations are quite different, not only in the actual cloud amounts but also in important derived quantities such as surface energy fluxes and precipitation. This sensitivity experiment covering an entire year demonstrates the important fact that many aspects of a re-analysis are to a high degree defined by the assimilating forecast model, and particularly by its physics. The difference between the annual averages of the daily mean total cloud amounts are shown in Figure 5. The prognostic scheme

produces more low clouds over the oceanic storm tracks and near the equator, while the Arctic Stratus are reduced. These are improvements. A negative impact is the reduction of low level Stratus and Stratocumulus over the up-welling Benguela, Humboldt and California currents. At the Cirrus level the new scheme produces more clouds over the tropical convective areas.

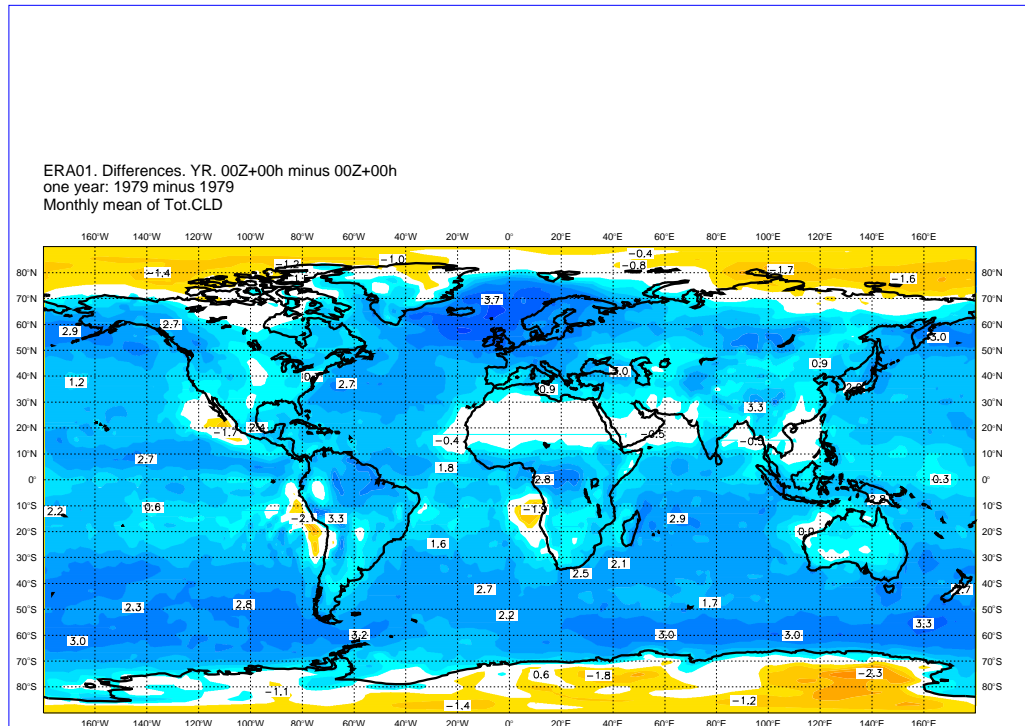


Figure 5 - Difference, in octas, between the annual mean total cloud cover from the prognostic and diagnostic cloud schemes. Blue colours indicate more total cloud in the prognostic (ERA) scheme

As a consequence of the changes in clouds, soil moisture, oceanic albedo and shallow convection, large differences also appear in the surface energy exchanges. Over the storm track latitudes the revised scheme feeds  $20\text{-}30\text{ W/m}^2$  more long wave radiation into the ocean. This is presumably closely related to the increase of low level clouds. The short wave radiation flux into the sea at low latitudes is reduced due to the increased clouds and the revised albedo. The evaporation from the tropical oceans is also affected; expressed as latent heat flux the reduction exceeds  $10\text{ W/m}^2$  over large areas, locally up to  $30\text{ W/m}^2$ . The overall net effect on the annual surface energy budget is seen in Figure 6. There is more energy input to the ocean in the tropics (except over the Pacific counter-current), and also over the high latitude storm tracks.

ERA01. Differences. YR. 00Z+24h minus 00Z+24h  
 one year: 1979 minus 1979  
 Monthly mean of Net Flux

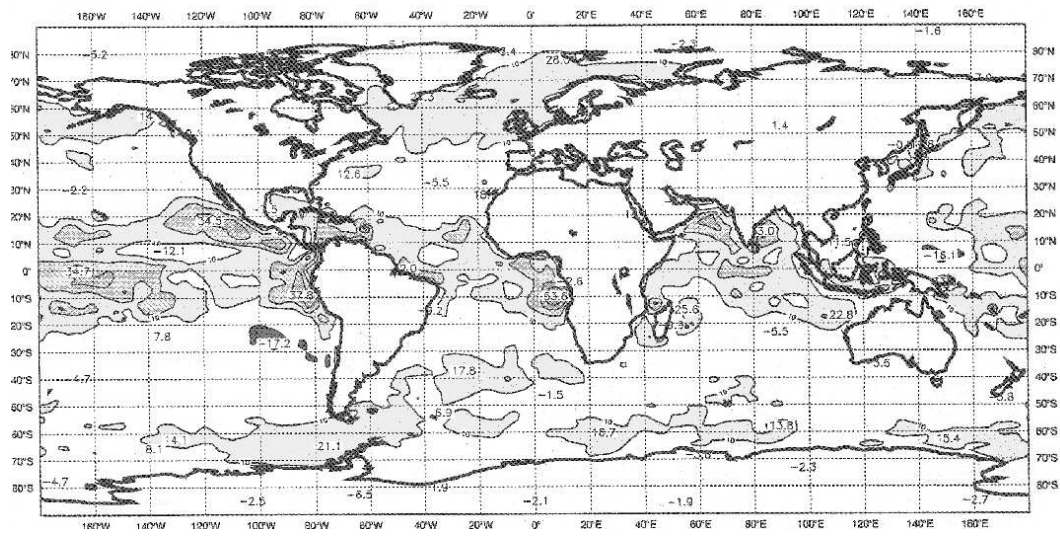


Figure 6 - Difference in  $W/m^2$  between the annual mean surface net energy fluxes from the prognostic and diagnostic cloud schemes. Positive values indicate LESS energy loss from the surface to the atmosphere

## 5. The ECMWF Re-Analysis Data Assimilation Scheme

From the experiences described in 4. above the following data assimilation system was selected and used for the 15 years of re-analysis.

- Spectral T106 resolution with 31 vertical hybrid levels.
- Intermittent statistical (optimum interpolation) analysis with 6 hour cycling and noFGAT.
- One dimensional variational (1D-VAR) physical retrieval of TOVS cloud cleared radiances below 100hPa, and NESDIS operational retrievals above. No TOVS data were used above 100hPa between 20°N and 20°S.
- Diabatic, non-linear normal mode initialisation, five vertical modes.
- The Integrated Forecast System (IFS) version of the ECMWF forecast model with 3-dimensional semi-Lagrangian advection.
- Mean orography with a compatible parametrization of the effects of sub-grid scale orography.
- Prognostic soil temperature and soil moisture, with nudging of the moisture from boundary layer atmospheric humidity analyses.
- Prognostic equations for cloud water and ice content and the cloud cover.
- ECMWF operational radiation parametrization with prescribed concentrations of aerosols, CO<sub>2</sub> and O<sub>3</sub>, with O<sub>3</sub> varying geographically and seasonally, the aerosols varying geographically and vertically and the CO<sub>2</sub> held constant.
- ECMWF operational planetary boundary layer parametrization.

The externally prescribed forcing of the re-analyses, in addition to the observations, comes from the ocean surface temperatures (SST) and the ocean ice cover, and has been described in section 3.2 on page 11 above.

Apart from the horizontal resolution, the ERA assimilation system was identical to the ECMWF operational system used between April 1995 and January 1996.

The principal components of the scheme are the one dimensional variational analysis of the cloud cleared radiances, the optimal interpolation analysis, and the global atmospheric model. In the following some aspects of these components as used in ERA are presented. Particular emphasis has been placed on aspects of the system which do not accord strictly with the scientific documentation presented in ECMWF's Research Manuals (ECMWF, 1992). For in-depth descriptions of the components of the ECMWF data assimilation and forecast the reader should consult the Research Manuals, and the bibliography provided (page 67).

## 5.1 One dimensional variational analysis (1D-Var)

A scheme developed by Eyre to make use of the raw TOVS radiances had been adapted at ECMWF to run on cloud cleared radiances and is known as “one-dimensional variational analysis” or 1D-Var. Integral components of the scheme include a radiative transfer model and a radiance bias monitoring and tuning scheme. Within the 1D-Var process a comprehensive quality control is performed on the radiances (Eyre, 1989, 1992, 1993; Eyre et al. 1993).

In the re-analysis 1D-Var is applied globally, including the use of the three stratospheric channels of the SSU.

### 5.1.1 The 1D-Var method

The variational part is to find the atmospheric temperature and humidity structure (1D-Var retrieval) which best fits the measured radiances. It is achieved by the minimization of the penalty function with respect to the atmospheric state, which is the fit of the measured radiance vector to the atmospheric state vector in radiance space (calculated by the radiative transfer model), to the background profile and to other information. The method of Newtonian iteration is used to minimize the penalty function starting from the first guess as the initial profile. If a sounding has not converged within 5 iterations it is rejected. TOVS channels used by the 1D-Var are: HIRS channels 1-7 and 10-15, MSU channels 2-4 and SSU channels 1-3 are used for “clear” and “partly cloudy” soundings; HIRS channels 1-3, MSU channels 2-4 and SSU channels 1-3 are used for “cloudy” soundings. A sounding is also rejected even if the minimization converges if the “measurement cost” for any channel exceeds its threshold value. A sounding is rejected due to residual cloud contamination if the measured-minus-forecast difference for HIRS 10 is below the threshold values over sea, over sea-ice and over land. In the stability check, based on the results by Andersson, a number of retrievals with suspected erroneous static stability are rejected (Andersson et al., 1991). Finally the accepted retrievals are thinned to a spacing of about 250 km (Eyre et al., 1993).

An important contribution to the ERA humidity analysis is derived from the 1D-Var assimilation of the radiance information contained in especially the “water vapour channels”, HIRS channels 10, 11, and 12 (McNally and Vesperini, 1996).

### 5.1.2 Bias corrections for 1D-Var

Eyre points out that for the effective implementation of 1D-Var it is necessary to apply a bias correction to the CCR data (Eyre, 1992). The “measurements” (CCR data) have undergone calibration and preprocessing. Any radiative transfer model has random and systematic errors. The systematic errors mainly result from the errors in the spectroscopic data, on which the radiative models are based. Within the 1D-Var process the radiative transfer model is applied to forecast model profiles. The differences between the measured and the



calculated brightness temperatures contain components from errors in the preprocessing of raw radiances, the radiative transfer model and the forecast model. The magnitude of the bias is of the order of a typical forecast error that the radiances try to correct; thus it has to be removed. Before 1D-Var retrievals are “actively” produced from a new satellite, the 1D-Var processing is done in “passive” mode producing the departure statistics without the final 1D-Var retrievals to allow the calculation of the initial biases. The passive period is typically two to four weeks, and has guaranteed a smooth transition to new satellites.

As pointed out by Eyre it would be preferable to correct these errors at source, but since this is not possible a practical strategy has been adopted (Eyre, 1992). Biases between measured brightness temperatures and those calculated from the six hour forecast profiles are adjusted using corrections calculated from the previous months biases close to a selection of reliable radiosonde stations in different parts of the world. The bias corrections are determined for each channel and are then applied during the following month of assimilation.

For quality control purposes the mean corrected and uncorrected measurement minus first guess departures for each six hour period are plotted against time as a monthly “radgram” for each channel and satellite. Since the first guess itself is independent of any changes in the CCR data, at least when a change is about to happen, these graphs reveal satellite problems that have occurred during the previous month. Often NESDIS has listed a change (e.g. a change in the water vapour attenuation coefficients), but it is only afterwards that it can be seen whether or not this change has caused a significant problem in the data assimilation. In practice full use of this information would require the bias tuning to be done separately during all the abnormal periods, and those periods subsequently re-run with new coefficients.

### **5.1.3 The use of retrievals in the analysis**

In the Optimum Interpolation analysis the 1D-Var temperature retrievals are used globally below 100 hPa over sea areas; they are not used over land. In the tropics only cloud free retrievals are used. The NESDIS temperature retrievals are used above 100 hPa in the extra-tropical areas of both hemispheres. In the tropics no retrievals are used above 100 hPa. Humidity retrievals are used below 300 hPa over sea areas, and are not used over land. Figure 7 gives a diagrammatic picture indicating which kind of retrievals are used where. All retrievals are subjected to further quality control within the OI analysis system, together with all other observations, before use.

## **5.2 The analysis**

In contrast to some other analysis schemes, grid points are not analysed individually in the ECMWF system but are grouped together, in “boxes” of variable horizontal size depending on the data density. The boxes

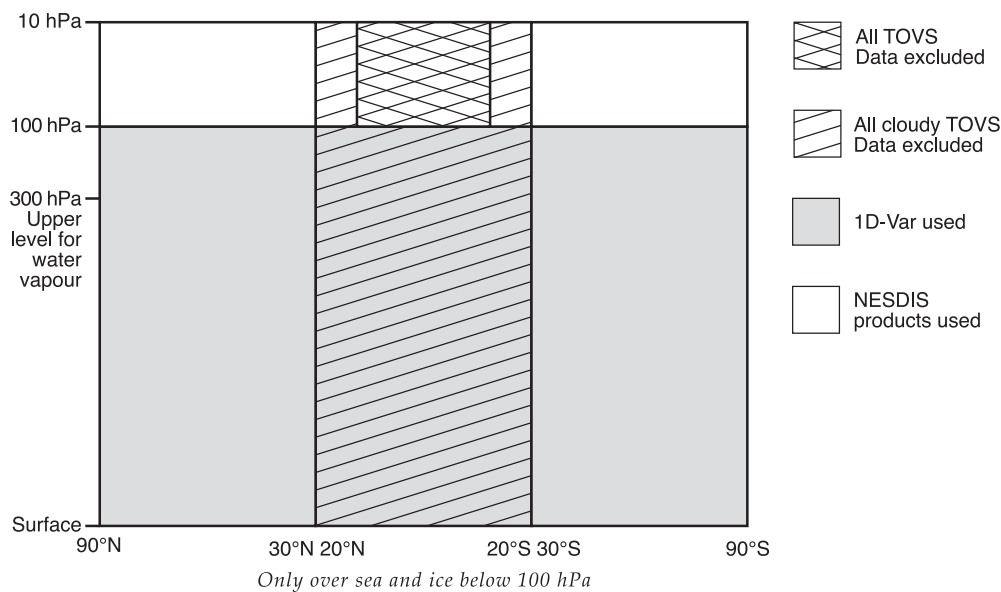


Figure 7 - The use of TOVS retrievals in the ERA analyses

extend from the surface to 100 hPa and from 300 hPa to the model's top level. The analysis for all the grid points in each box is carried out using the same data from the box and surrounding boxes, assuring consistency of the analysis between the grid points. The analysis is evaluated on the model levels, not on standard pressure levels. For a comprehensive description of the analysis system used see ECMWF (1992), Shaw et al. (1987), Lönnberg (1988), and Undén (1989)

### 5.2.1 Monitoring, bias correction, and observation blacklists

For each item of observed data which is processed by the ECMWF analysis a comprehensive set of difference information is computed. These include the difference between observed and analysis (OB-AN), observed and initialised analysis (OB-IA), and observed and first guess (OB-FG) values. This information, together with the observed values, the quality flags, and the processing flags is called "analysis feedback", and is the source material for much of the monitoring. A further statistic extensively used for monitoring purposes is the set of increments added to the first guess to produce the analysis (AN-FG). Figure 8 illustrates the values on which the difference information contained in the analysis feedback are based.

#### Radiosonde data

In ECMWF operations a comprehensive system for the correction of systematic errors in radiosonde temperature and geopotential is used. It is based on feedback information from the data assimilation and determines corrections, which are a function of the solar elevation, to individual radiosonde observations made by known instrument types. A simplified version of this scheme has been adapted for ERA. During

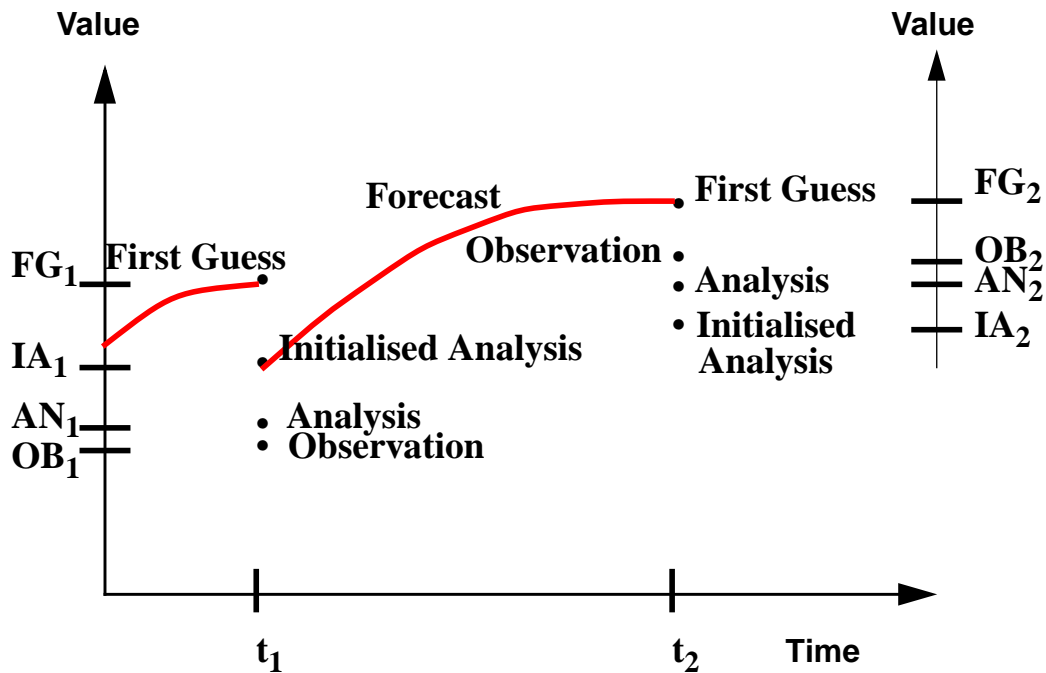


Figure 8 - Difference information contained in “analysis feedback”.

most of the re-analysis period the actual radiosonde type used is not available in the database. In consequence bias corrections are calculated only for those WMO blocks where homogeneous radiosonde equipment was believed to have been used. Measurement minus first guess departures from the preceding twelve months are used to cover all the possible solar elevations. Only 20% of the calculated bias is applied for the observed height at 300 hPa; 40% and 80% are applied at 250 hPa and 200 hPa levels respectively. Above 200 hPa the full correction is applied. The corrections calculated and used for 1980 were also applied in the 1979 rerun.

In order to decide which stations should be corrected the analysis feedback information and monthly mean analysis increment (AN-FG) fields were monitored. A large mean increment can result from model problems (for example when the increment is downstream of a data sparse area), from systematic instrument errors, or from errors in observational practice. If the station characteristics are not represented accurately in the model (for example a station in the vicinity of locally steep orography) this can also result in large increments at nearby levels. After considering these effects areas with suspicious stations are added to the bias correction scheme, and individual stations with very large first guess deviations are added to the blacklist. The monitoring is applied both to the uncorrected and corrected observations so that stations can be removed from the correction list and from the blacklist when their quality improves. There is thus a continuously evolving radiosonde bias correction and blacklisting. The bias correction was more important during the first

half of the re-analysis. Noticeable improvements in the quality of radiosondes later in the re-analysis period resulted in a marked reduction in the corrections which needed to be applied.

### **Other observational data**

Very few stations other than radiosonde stations were included within the blacklist. A notable exception is a number of SYNOP stations near the Andes in Western South America, to the West of the Amazon basin. The surface pressure data from these stations, coupled with their temperature and humidity data were found to produce a spurious drying out of the surface moisture, due to deficiencies in the way they and the adjacent steep orography were handled by the system. Blacklisting the surface pressure of a selection of these stations was used as a crude “cure” for this problem.

### **5.2.2 The analysis and quality control**

The analysis itself is used to perform quality control on the observations. During a first pass through the analysis, the observed values are compared with each other and with the appropriate data from the 6 hour forecast used as a first guess to generate a quality assessment of the data they contain, and to select the most appropriate values for use within the analysis proper. Stations which report more than once during the 6 hour period or appear in duplicate form are reduced in number, the observation closest to analysis time being chosen. High density aircraft data and drifting buoy data are thinned where necessary. There are specific checks for multi-level data. An observation which has been rejected in the early stages cannot be considered in later checks. Observations accepted in the early checks can later have their quality re-assessed, and possibly be rejected.

Data from TEMPs are normally only taken from 15 standard levels. If any are missing the nearest significant level will be used. The heights to the significant levels have been computed during the hydrostatic check. If there is a significant difference between a reported standard level and the re-computed one, the former will be rejected and the latter used.

### **5.2.3 The assumed observation errors ( $\sigma_0$ )**

In the ECMWF analysis system all observations of the same type are ascribed a typical error variance ( $\sigma_0$ ), computed from a long series of observations compared with analysis. Except for TEMPs, there is generally no distinction between different platforms, all are assumed to be of equal quality.

The assumed typical wind errors are for SYNOP/SHIP: 3-4 m/s, DRIBU 5-6 m/s. TEMP and PILOT are assumed to have a typical error of 2-3 m/s in the lower troposphere, compared to 3 m/s for AIREP and

SATOB. In the upper troposphere TEMP and PILOT are assumed to have errors around 3 m/s, AIREP 4 m/s and SATOB 6 m/s.

The assumed typical height errors are for SYNOP 7 m (1 hPa), SHIP and DRIBU 14 m (2 hPa) and PAOB 32 m (4 hPa). For TEMP there are three quality classes, defined according to the monitoring statistics. The typical 200 hPa geopotential error in the first group is 13 m, in the second 20 m and in the third 26 m.

Certain vertical error correlations are used to “spread out” the influence of, for example, an observation of an AIREP in the vertical. Thus a wind report at 250 hPa is assumed to correlate 0.5 with the wind at 200 and 300 hPa, only 0.1 with 500 hPa and 100-150 hPa. In the same way a height observation at 500 hPa is assumed to correlate around 0.5 with the height at 700 and 350 hPa.

#### 5.2.4 The assumed “First Guess” (FG) errors ( $\sigma_g$ )

The assumed uncertainty of an observation ( $\sigma_o$ ) is combined with the assumed uncertainty of the FG ( $\sigma_g$ ), resulting in an estimate of the total uncertainty in the analysis. For the following FG 6 hours later this uncertainty is increased by about 50%, a value roughly representative of a typical error growth over six hours.

In the ERA analysis system, neither the analysis error nor the FG error are flow dependent. They depend to a large extent on the typical data quality and coverage in the area, which in some areas may lead to occasional misfits.

#### 5.2.5 Objective optimum interpolation analysis

If  $Z_g$  is the extrapolated geopotential (or FG) and  $Z_o$  a single new observation,  $\sigma_g$  and  $\sigma_o$  are the assumed errors, then the analysis  $Z_a$  takes the value

$$Z_a = Z_g + (Z_o - Z_g)\sigma_g^2 / (\sigma_o^2 + \sigma_g^2)$$

which means that when the observations are unreliable,  $\sigma_o$  is large and  $Z_a$  almost takes the value  $Z_g$ . Then there is little impact on the FG. On the other hand, when the observations are assumed fairly accurate,  $\sigma_o$  is small and  $Z_a$  almost takes the value  $Z_o$ . Then the observations will have a substantial impact on the analysis.

The ECMWF “Optimum Interpolation” (OI) analysis method is an extension of optimal interpolation (Eliassen, 1995, and Gandin, 1963) to a multivariate three dimensional interpolation of deviations of observations from a forecast field (Lorenc, 1981). It is more correctly “statistical interpolation” since assumptions

made in using linear regression and error covariance when modelling the interpolation result in a process which is not truly optimal.

### 5.2.6 Snow cover

The snow cover is initialized at every analysis time from a combination of two fields, snow fall and snow depth, both analysed with a simple successive correction method. The snow fall analysis is based on station snow fall data and the snow depth analysis on persistence, observed station snow depths and climatology. Satellite-based snow cover estimates were not used in ERA. The amount of snowfall and snow depth observations vary considerably during the ERA years, there were for instance very few observations from central Asia and Siberia before 1992.

It is important to point out that since the snow cover is analysed from observations, the water mass budget of the hydrological cycle is not closed for the snow phase.

### 5.2.7 Soil Moisture

The soil moisture is initialized at each analysis time by a very simple nudging method based on the analysis increments in the near surface atmospheric humidity. The vertically integrated soil moisture in the three upper layers is corrected at each analysis time by a correction term proportional to the humidity analysis increment (Viterbo and Courtier, 1995, Mahfouf, 1991)

$$\Theta_a = \Theta_g + C\Delta t(q_a - q_g)$$

Where  $\Theta$  is the integrated soil moisture and  $q$  the near-ground atmospheric humidity.  $C$  is a constant and  $\Delta t$  the time step. Subscripts  $a$  and  $g$  stand for analysis and first guess respectively.

### 5.2.8 The normal mode initialisation

Though the wind and mass fields are balanced within the analysis “boxes”, on the larger scale and away from the equator, minor imbalances still appear between the “boxes”. These imbalances set up fictitious, undesired gravity waves. In the normal mode initialisation process the model suppresses these gravity waves. During the process, the mass and wind fields become adjusted in such a way that no further undesired gravity waves will appear.

A primary reason for initialisation is to improve the data assimilation. Unless initial, spurious waves in the first guess forecast, especially in the surface pressure, are eliminated, they can lead to the rejection of good,

and the acceptance of bad observations, and to a degraded estimation of the necessary increments to be generated by the selected observations.

## 5.3 The ECMWF global atmospheric model

### 5.3.1 The model formulation

The model characteristics can be summarized by six basic physical equations, the resolution in time and space and the way the numerical computations are carried out. A detailed documentation of the ECMWF forecast model is under preparation, and will be available on the Internet. A description of the numerical aspects and the semi-Lagrangian implementation can be found in Ritchie et al. (1995).

### 5.3.2 The basic equations

Of the six equations governing the ECMWF primitive equation atmospheric model, two are diagnostic and tell us about the static relation between different parameters:

- The GAS LAW gives the relation between pressure, density and temperature,
- The HYDROSTATIC EQUATION shows the relationship between the density of the air and the change of pressure with height,

The other four equations are prognostic and describe the changes with time of the horizontal wind components, temperature and water vapour content of an air parcel, and of the surface pressure.

- The EQUATION OF CONTINUITY ensures that the mass is conserved and makes it possible to determine the vertical velocity and change in the surface pressure.
- The EQUATION OF MOTION describes how changes in the wind are caused by the mass gradient, the Coriolis force and what the effects of friction are near the earth's surface. The wind field is described in the model by its vorticity and divergence, which are the forecast variables. The west- and south-wind components are extracted at the post-processing stage
- The THERMODYNAMIC EQUATION expresses how a change in temperature is brought about by adiabatic cooling or warming due to vertical displacement, latent heat release, radiation from the sun, the air and the earth's surface and frictional or turbulent processes (diffusion).

- The CONTINUITY EQUATION FOR MOISTURE assumes that the moisture content of an air parcel is constant, except for losses due to precipitation and condensation or gains by evaporation from clouds and rain or from the oceans and continents.

The hydrostatic assumption eliminates vertically propagating sound waves. Gravity waves, (and strictly horizontal sound waves) are retained by the primitive equations. A proper treatment of the gravity waves is essential for the adjustment processes between mass and wind.

### 5.3.3 The resolution in time and space

#### Temporal resolution:

The computational time step has to be chosen with care in order to avoid numerical instabilities and ensure sufficient accuracy. The re-analysis system used a time step of 30 minutes.

#### Vertical resolution:

The atmosphere is divided into 31 layers. The resolution (measured in geometric height) is highest in the planetary boundary layer, where the levels follow the earth's surface, lowest in the stratosphere where they coincide with the pressure surfaces. In between a smooth transition is applied. Table 4 lists values of pressure at each of the 31 model levels when the surface pressure is 1015 hPa, while the 31 level resolution is shown schematically in figure 9.

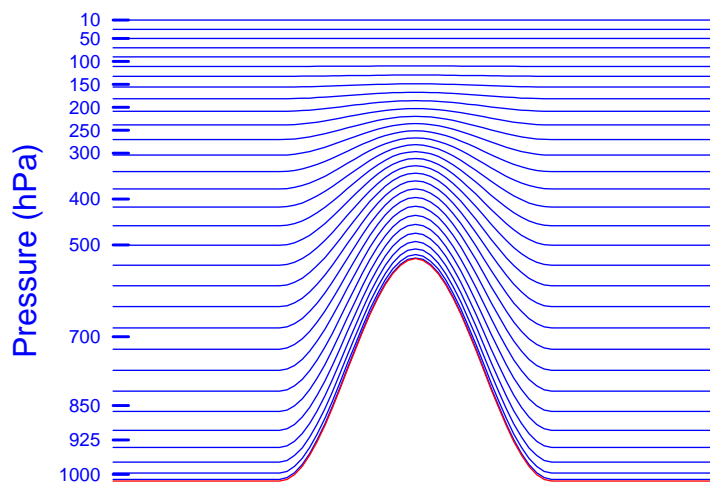


Figure 9 - The 31-level vertical resolution



**Table 4 - Pressure of model levels when the surface pressure is 1015 hPa**

|    | (hPa) |    | (hPa) |    | (hPa) |
|----|-------|----|-------|----|-------|
| 1  | 10    | 11 | 238   | 21 | 634   |
| 2  | 30    | 12 | 270   | 22 | 681   |
| 3  | 50    | 13 | 304   | 23 | 727   |
| 4  | 70    | 14 | 340   | 24 | 773   |
| 5  | 90    | 15 | 378   | 25 | 819   |
| 6  | 110   | 16 | 417   | 26 | 863   |
| 7  | 132   | 17 | 458   | 27 | 904   |
| 8  | 156   | 18 | 501   | 28 | 942   |
| 9  | 181   | 19 | 544   | 29 | 973   |
| 10 | 209   | 20 | 589   | 30 | 997   |
|    |       |    |       | 31 | 1011  |

### Horizontal resolution

The ECMWF model uses two different horizontal numerical representations:

- a spectral representation, based on a triangular truncation at wave number 106 (T106), for the representation of upper air fields and the computation of the horizontal derivatives,
- a grid point representation used for computing non-linear adiabatic terms and the diabatic physical parametrization.

The spectral technique, where the wave-like atmospheric features are represented by trigonometrical functions, is more efficient than the grid-point technique. Though the grid can describe features with half a wavelength down to 1.2 degrees, due to numerical reasons the waves would have to be twice as long to be properly advected by a finite difference scheme. In this sense the grid point representation is coarser than the spectral representation, which has an effective resolution of about 1.6 degrees.

It is convenient to integrate spectral models by carrying out much of the computation on a so-called Gaussian grid, which is regular in longitude and almost regular in latitude. Due to the convergence of the lines of longitude toward the poles, the east-west distance between the grid points decreases towards the poles. At 60° latitude it is half that of the equator, in the polar region north of 80° latitude it is less than 1/20 compared to the equator. This very dense east-west resolution, not matched by a similar resolution along the north-south direction, takes more computer time than is necessary for accuracy. To save computer time, a reduction

of the Gaussian grid was introduced in 1991. The reduced Gaussian grid is defined as a step-wise reduction of the number of grid points along a latitude line, to keep the east-west separation almost constant. Between 20N and 20S the grid is identical to a regular Gaussian longitude-latitude grid. By doing this the computational time has been reduced by about 25 to 30%.

### 5.3.4 The numerical formulation

The choice of a numerical scheme is the result of a compromise between the need to preserve numerical accuracy, and the need to save computer time and speed up the forecast. When the operational T213L31 model was implemented in 1991, the traditional Eulerian scheme would have been too expensive, and a semi-Lagrangian scheme was introduced to reduce the computer cost.

The basic difference between an Eulerian and a Lagrangian representation can be seen from the equation (in one-dimensional space)

$$\frac{dQ}{dt} = \frac{\partial Q}{\partial t} + U \frac{\partial Q}{\partial x} = 0$$

which in an Eulerian way expresses that the local changes in  $Q$  are due to the advection of  $Q$  by the wind  $U$ :

$$\frac{\partial Q}{\partial t} = -U \frac{\partial Q}{\partial x}$$

or in a Lagrangian way that  $Q$  is conserved for a given parcel

$$\frac{dQ}{dt} = 0$$

Whereas most Eulerian schemes require small time steps to avoid numerical instability, (the quantity  $Q$  must not be advected by more than one grid length per time step), the Lagrangian scheme allows longer time steps, where a limitation is the need to approximate curved trajectories by straight lines (or great circles on the globe) during each time step.

Although it would be possible in theory to carry out predictions in a Lagrangian framework by following a set of marked fluid parcels, in practice shear and stretching deformations tend to concentrate parcels inhomogeneously, so that it is difficult to maintain uniform resolution over the forecast region. A semi-Lagrangian scheme is used to overcome this difficulty.

In this version, the grid points are stationary. At each time step the scheme computes a backward trajectory from every grid point. The point reached defines where the air parcel was at the beginning of the time step.

The value of the variable in that point is then carried forward to the grid point, applying the various physical processes.

### **5.3.5 Parametrization of physical processes**

The primary purpose of the ECMWF model is medium-range weather forecasting, which has been defined as the production of operational weather forecasts for the time-range 4-10 days. Although the purpose of the re-analysis is different, using the same system has many benefits. Either goal requires very good descriptions of the various physical processes that affect the weather development. A ten-day integration makes it absolutely necessary to include effects with relatively long time scale, even as subtle as the evaporation by vegetation, in order to handle the flow pattern more accurately. The different time scales and feed-back mechanisms between the various processes makes the computations complex and expensive.

The mechanisms for these processes are mainly related to small scale disturbances in space and time, smaller than the scales explicitly resolved by the model, from convective clouds down to molecular processes. The effect that these sub-gridscale processes have on the larger scales can be computed only by parametrization, i.e. formulating indirectly their overall effect in terms of known grid scale variables.

#### **The Planetary Boundary Layer**

The treatment of the planetary boundary layer (PBL), the lowest part of the troposphere, plays a fundamental role for the whole atmosphere-earth system. It is through the surface exchanges of momentum, heat and moisture that the atmosphere “feels” that it moves over a rough land surface or a wet smooth sea.

In the ECMWF model the lowest six levels are at around 30, 140, 340, 600, 900 and 1200 m above the model surface. Even with this fairly high resolution the vertical gradients of temperature, wind, moisture etc. in the PBL cannot be described very accurately, let alone the turbulent transports of momentum, heat and moisture. For the estimation of these parameters the model uses the larger scale variables such as wind, temperature and specific humidity, with the assumption that the transports are proportional to the vertical gradients. At the earth’s surface, the turbulent transports of momentum, heat and moisture are computed as functions of air-surface differences and surface characteristics. This approach is often referred to as first order turbulence closure, in contrast to so called higher order schemes where the turbulence is predicted explicitly in one form or another.

#### **The surface**

The model orography determines the relief of the lower model boundary, but other characteristics such as vegetation, snow cover, sea ice distribution, albedo &c. strongly influence the surface processes in the model.

To have a realistic simulation of the boundary layer, the knowledge of such factors as the heat and moisture content in the surface soil is essential. The degree to which convective clouds are created in the model depends on the stored heat and moisture in the soil. Over land areas, snow depth, soil temperature and soil wetness are forecast variables, calculated by a model of the soil with 4 layers at depths 7, 21, 72 and 189 cm. Over the sea the surface temperatures are prescribed by external analyses

### **The orography**

The ERA orography is given by a spectral T106 fitted version of the gridpoint averages (in the model resolution) of a  $1/6^\circ \times 1/6^\circ$  reference field. This field is referred to as the ‘mean’ orography and is supplemented by four additional fields describing the height, orientation, anisotropy and slope of the sub-grid orography. This allows a realistic representation of the mountain drag. An important part of the scheme is that, depending on dynamical criteria, it can block the low level flow rather than make the air go over the orography.

Compared to older versions of the orography parametrization, the ERA mean orography, together with the physical parametrization, produces more realistic precipitation in mountainous regions; whereas in the older versions the largest rainfall tended to fall on the tops of mountain ranges, it now falls on the slopes.

### **The land-sea mask**

The model surface is logically divided into sea and land points. A grid point is defined as a land point if more than 50% of the actual surface of the grid is land, calculated from the  $1/6^\circ \times 1/6^\circ$  reference field.

### **Sea surface temperature and sea-ice**

The sea surface temperature (SST) used in ERA is taken from analyses produced externally, as described in section 3.2 on page 11. The SST of ice-free water was kept constant during the 24-hour and 10-day forecasts. There is no separate field in ERA describing the sea-ice distribution; instead it is defined as sea points with SST values below  $-1.8^\circ\text{C}$ . The temperature at the surface of the ice is variable, according to a simple energy balance/heat budget scheme. The distribution of sea and sea-ice points is kept constant during the forecast; no freezing of the water or melting of the ice is allowed.

### **Albedo**

A background yearly climate field is used, according to which the albedo is set to 0.55 over sea ice and 0.07 over open water. Over land the albedo has a minimum value of 0.07 and cannot exceed 0.80. The model is able to alter it during the run according to changes in snow cover, but not to changes in vegetation.

### **The soil representation**

The parametrization of the surface processes over land takes into account the distribution between bare land and vegetation (based on geographical data) at each grid point. The soil is represented by a four-layer model with layers at depths 7, 21, 72 and 189 cm. as described earlier. The soil hydrology is simulated in the same four layers. A skin (or brightness) temperature, characteristic of a layer with no heat capacity at the soil-atmosphere interface, represents the balance between radiative fluxes, sensible and latent heat fluxes and a flux into the ground. Temperature in the four soil layers changes due to the combined effect of ground heat flux and snow melting, where appropriate.

### **Snow cover**

The thermal properties of snow covered ground depend only on the depth of the snow cover (actually the amount of water in the snow). No considerations are made for the age of the snow, i.e. the model will treat old dark snow as if it was white.

### **Soil moisture**

The soil moisture is divided into skin and soil reservoirs. The skin reservoir (which mainly is moisture on vegetation) evolves under the action of its own evaporation and its ability to collect dew and intercept precipitation. The soil reservoir takes into account contributions from precipitation and snow melt, as well as losses due to deep penetration (gravity), evaporation over bare ground and root uptake by vegetation (i.e. to the transpiration). Vegetation uptake takes place in the three upper layers, the root depth. The soil moisture budget is not closed, excesses are removed as ‘run-off’ which has been extracted and is available as an ERA product. The run-off contains three parts, surface run-off, deep penetration and excess over saturation in each layer. The surface run-off is the difference between the throughfall (where throughfall = precipitation - interception on vegetation) and the infiltration into the soil. The deep penetration is the dominant component of the run-off

### **Further climatological fields**

The fraction of vegetation is specified in each grid point and used by the model to estimate the roughness and the evaporation. This field does not vary with the seasons.

### **Gravity wave drag**

When stably stratified air flow crosses a mountain ridge, gravity waves are excited in the flow. Depending on the static stability and vertical wind shear, these gravity waves can propagate vertically until they have sufficiently large amplitude to break. This process has a certain impact on the large scale flow; it makes it slightly less zonal and contributes to the formation of blocking highs and cut-off lows. This physical process is incor-

porated into the model as the gravity wave drag (GWD) scheme. It represents the momentum transport due to sub-grid gravity waves. Some of the wave drag occurs in the stratosphere, and there is also significant low-level drag. The dependence on static stability and wind speed implies a maximum in winter and a minimum in summer.

## **Radiation**

In view of the importance of cloud-radiation interaction in both long and short term processes, ECMWF has placed high emphasis on the treatment of the absorption and scattering by clouds of solar and terrestrial radiation. About one fifth of the overall computational time in the forecast model is devoted to the radiation scheme, as much as for the dynamics.

The radiation spectrum is divided into eight frequency bands: two in the short wave spectrum (direct and diffuse radiation from the sun), and six in the long wave spectrum (from the earth and within the atmosphere). The upward and downward diffused radiation is computed for each of the eight spectral bands. The parameters influencing the emission and absorption are pressure, moisture, cloud cover and cloud water content. Assumed parameters are the ground albedo (modified according to the snow cover), the solar constant and the concentration of CO<sub>2</sub>, O<sub>3</sub> and aerosols. The solar constant has the value 1370 W/m<sup>2</sup>. The carbon dioxide has a constant mass mixing ratio over the whole globe corresponding to a volume concentration of 353 ppm(v). The ozone distribution depends on height, latitude, longitude and season, based on analyses from the 1970's.

The radiation scheme is designed to take the cloud-radiation interactions into account, in considerable detail. It allows partial cloud cover in any layer of the model. For cloudy grid points, computations are made both for clear and overcast conditions, and the total amount weighted together according to the forecast cloud amount.

## **Convection**

The convection schemes in the model (Tiedtke, 1989) fulfil five objectives:

- creation of cloud amount to be used by the radiation scheme,
- computation of precipitation,
- computation of vertical transport of moisture,
- computation of vertical momentum fluxes,

- computation of temperature changes in the atmosphere due to release of latent heat or cooling in connection with evaporation.

In the general convection scheme, sub-grid vertical fluxes of mass, heat, water vapour and momentum are computed at each model level with the help of a simple cloud model interacting with its environment. The scheme is applied to penetrative convection, shallow convection and mid-level convection. They are mutually exclusive, so only when the scheme fails to create cloud of one type, does it try the next.

Deep convection predominantly occurs in disturbed situations with a deep layer of conditional instability and large-scale moisture convergence. The down draught mass flux is assumed proportional to the up draught mass flux.

Shallow convection predominantly occurs in undisturbed flow, in the absence of large scale convergent flow. For example trade wind cumuli under a subsidence inversion, convection occurring in the ridge region of tropical easterly waves or day time convection over land. The moisture supply is from surface evaporation. It does not normally produce precipitation.

Mid-level convection describes convective cells which originate at levels above the boundary layer. A well known example is *Altostratus castellanus floccus*. Less clearly visible, but frequent, are rain bands connected to extra-tropical cyclones.

## Clouds

There is no analysis of clouds, but the 6-hour first guess forecast clouds are carried forward to the next analysis time. Although in general the forecast cloud cover gives useful information, the main purpose of the cloud scheme is to provide input to the radiation computations.

In the ERA model the clouds are described by three prognostic parameters: the cloud fraction, the content of cloud liquid water and cloud ice. The cloud scheme is unique in treating the main cloud-related processes in a consistent way by forecasting both cloud fraction and cloud water/ice content with their own prognostic equations. The cloud processes are strongly coupled to other parametrization processes. (Tiedtke, 1993; Jakob, 1994)

Clouds are generated by large-scale ascent, cumulus convection, boundary layer turbulence and radiative cooling. They are dissipated through evaporation due to large-scale descent, cumulus-induced subsidence, radiative heating and turbulence at both cloud tops and sides, as through precipitation processes.

Convective clouds are computed in parallel with the convective scheme (see above). Moisture is carried upward and condenses into liquid water/ice or “condensate”. This condensate will either fall out as precipi-

tation, be carried higher up in the cloud or be advected horizontally out of the cloud. In this latter case, and only then, the scheme will use this part of the condensate to create stratiform and cirrus clouds (altocumulus castellanus, anvils and other remains from convective processes).

Stratocumulus clouds are linked to the boundary layer moisture flux produced by the vertical diffusion scheme.

Stratiform clouds (e.g. low level stratus and medium level nimbostratus types) are determined by the rate at which the saturation specific humidity decreases due to upward vertical motion and radiative cooling.

Evaporation processes are accounted for in several ways: large-scale and cumulus-induced subsidence and radiative heating, evaporation at the cloud sides due to turbulent processes and turbulent motion at the cloud tops.

Precipitation processes take into account not only the local water/ice content, but also different precipitation enhancement processes. The effect of evaporation of falling precipitation is also included.

### **The hydrological cycle**

There are two precipitation generating mechanisms included in the ECMWF model, for convective and for stratiform (frontal or dynamical) precipitation. The generated precipitation is affected by evaporation and melting.

**Convective precipitation:** the condensation leading to precipitation is assumed to be liquid water or snow. No ice crystals or liquid water are assumed to be stored in clouds or floating in the air as cloud particles. The rain/snow partly moistens the atmospheric environment by detrainment, the rest falls out of the cloud as precipitation.

**Stratiform precipitation:** precipitation both as water and ice crystals (snow) are considered, depending on the temperature of the layer where condensation takes place. No condensation is stored as cloud drops or ice crystals. The transition from ice to water is supposed to occur when the precipitation passes through layers with temperatures warmer than +2°C. Freezing water is not considered in the model except as snow.

**Evaporation:** it is assumed that precipitation falling from a saturated layer saturates the first layer underneath before reaching the next layer below. This may substantially reduce the precipitation on the ground. Evaporation of the precipitation is not assumed to take place within the cloud, only between the cloud base and the ground. The layer below a precipitating, non-convective cloud is always almost saturated.



**Melting:** melting of falling snow occurs in a thin layer of a few hundreds of metres below the freezing level. It is assumed the snow can melt in each layer whenever the temperature exceeds 2°C. The melting is limited not only by the snow amount, but also by keeping the induced cooling of the layer such that the temperature of the layer after melting is not less than 2°C.

The three cloud parameters, cloud liquid water content, cloud ice water content and cloud fraction are extracted on the model levels and archived on the Gaussian grid. In addition there is an extraction of 'low', 'middle' and 'high' clouds, separated by the pressure levels 800 hPa and 450 hPa, these fields are also available as a 'more convenient' summary of the detailed cloud fields.

Again it is important to stress that the global hydrological cycle cannot be closed in a data assimilation such as ERA where the snow amount is adjusted each analysis cycle by observations (see section 5.2.6 on page 28).

## 6. Production

### 6.1 Overview

It was essential to develop a reliable production system capable of performing data assimilation at a very fast rate. Using the combined experience of the Centre's Operations and Research Departments, the systems in use were studied carefully, slimmed down where necessary, modified to exploit a data archive as opposed to real-time data, and optimised for performance. This resulted in a prototype system capable of performing at the required rate, which was further refined and completed while being used as the principal vehicle for the initial ERA experimentation.

A period of experimentation then followed to determine the exact components of the data assimilation system to be used for the full re-analysis. This has been described in some detail in section 4. on page 15.

Once production began, late in 1994, the scientific emphasis gradually moved from experimentation to monitoring and validation. The external forcing fields were validated before the production started by means of maps, averages and time series. Every effort was made to detect, as early as possible, potential problems which would require further investigation. Where appropriate, production was halted and re-started from an earlier date; in some cases production was allowed to continue, but the month or months concerned re-run at a later time. The production monitoring made use of a set of quality control tools, whose output, usually in the form of graphical information, was inspected continuously. All graphical and tabular monitoring results were kept both as hard copies and as files. Diaries were kept of all special events and problems encountered.

Production and monitoring continued throughout 1995 and into 1996. During the second quarter of 1996 the first pass through the full 15 years was completed. Monitoring enabled many errors which happened during the production to be located and rectified; nevertheless two lengthy periods needed to be re-run. First, the early production (to August 1980) was adversely affected by an error which significantly affected humidity at upper levels. Secondly, all cloud track wind data (SATOB) except the GMS data were accidentally excluded from June 1990 to October 1992, due to a change in their format within the ECMWF archive. A re-run of the first period was particularly desirable, as it presented an opportunity to run the FGGE year with the same observations and forcing fields as NCEP and DAO. Both re-runs were completed in September 1996.

The internal validation programme was augmented by the on-going work of the external validation projects. The continuous exchange of information between the ERA team and the validation partners proved to be extremely useful. It has resulted in material being available to potential future users of the data which should be of considerable assistance (ECMWF, 1997).

Close co-operation has also been established between the ERA team and the teams responsible for the NCEP re-analysis, and the re-analysis performed by the DAO.

## 6.2 Production system design

The design of the production system exploited the cost effectiveness of two SGI servers to which were attached a large amount of relatively inexpensive disk space, and attempted to optimise the locality of data to appropriate compute servers taking particular account of the type of connectivity.

The ERA production system ran under the control of ECMWF's Supervisor Monitor Scheduler (SMS) (Pesonen and Raoult, 1992). SMS enables computer "tasks" to be classified as belonging to "families" within "suites". Complex scheduling can then be performed according to attributes relating to events set by tasks, task completion, family completion, and various other criteria. Tasks may be designated to run on any known computer with a network connection to the computer on which the SMS is running. A graphical interface provides monitoring information, enables manual changes to be made when required, and gives fast access to task output, scripts, status information, and scheduling information. The use of SMS contributed greatly to the smooth and efficient running of the ECMWF re-analysis system.

The ERA production system comprised a number of modules, each of which was scheduled as an independent suite by the SMS. The various modules each addressed a specific part of the production for one month. They included modules to:

- extract and organize observational data,
- perform data assimilation,
- archive results,
- check each archive file, and to
- generate monthly means and statistics.

Figure 10 shows the principal concentrations of data associated with the main processing components together with their machine of residence. Data were moved from the Cray to the Silicon Graphics (SGI) environment as soon after creation as possible, minimizing the amount of Cray disk space needed. Within the SGI environment up to three months of observations and feedback, and up to two months of production fields could be accommodated. Data were added to the ECMWF's MARS archive as monthly files at the end of each month of production.

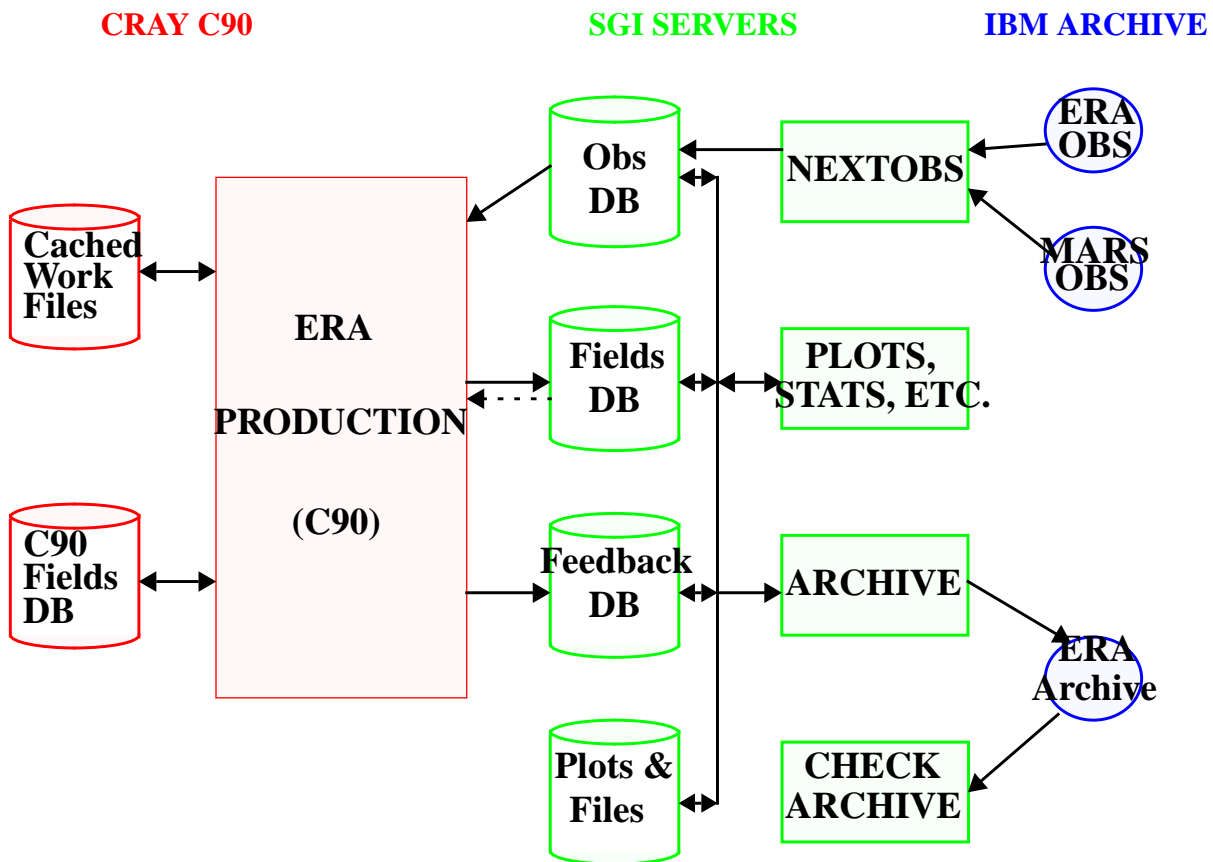


Figure 10 - principal concentrations of data associated with the main processing components of ERA.

Within the Cray C90 extensive use was made of the ability to cache data within a solid state storage device (LDCACHE). This ensured that files written by one process and subsequently immediately re-read by a subsequent process, and also small transient work files, were afforded highly efficient input/output. All sub-systems were broken up into small tasks which were then scheduled individually to achieve as much parallelism as possible.

### 6.3 Organising the observations

Two versions of this module have been developed - one to obtain the next month of observations from within the FGGE period, the other to perform the same task for the post-FGGE period. Observations were extracted to the SGI server, and inserted into an EMPRESS relational data base. All observations are represented in the WMO BUFR form used within the Centre's operational system.

A relational data base was used for this part of the processing to:

- assist with the identification of duplicate data;

- organize the data according to data type and data source;
- enable sub-sets of data to be defined and accessed quickly for investigative purposes.

EMPRESS was chosen because of its ability to represent data descriptive attributes in relational form while representing the associated data in pure binary form as binary large objects (BLOBs).

Especially in the post-FGGE period it has been found essential to load the observations into the data base in such a way as to ensure that the best version of each observation is retained, and other versions rejected. The order followed was: PAOB; buoys from COADS (these all have sensible identification numbers); GMS cloud winds; CCR; MARS conventional data, including ships; JMA TEMP and AIREP data; COADS ships; ships from MARS without proper call signs; ships from COADS without proper call signs.

Later data did not over-write earlier data for an identical date/time/location/ID combination. For SHIP data, the later data did not over-write earlier data for an identical date/time/location, with appropriate rounding of the time and location attributes (for duplicate identification purposes) to mask differences due to data having been encoded on different computers.

The MARS ships were given preference over COADS because they contain more data. The version of the COADS data set used only contains the basic surface parameters.

Frequent problems were encountered with respect to buoy data between the hours of 21:00 and midnight. It is suspected that, for many of these data, the date/time is in error by 24 hours. It has also been found that, in most cases where such discrepancies were noted, there were ample data for the midnight analyses from the buoys concerned between the hours of midnight and 03:00. In consequence no buoy data between the hours of 21:00 and midnight were added to the observations data base. When all buoys had been added, a check programme was run to produce monthly surface pressure profiles for each buoy, and to produce updates to the buoy blacklist.

When all data had been added to the observations data base a count was made for each observation type and each day. This was summarized within a monthly table, giving early warning of any deficiencies.

## **6.4 Data assimilation**

Figure 11 describes the main components of the ERA data assimilation module.

Observations were extracted as required from the observations data base. They were then subjected to a final modification process to ensure presentation to the assimilation system in an acceptable form. At this stage the corrections from the TEMP bias correction scheme were applied.

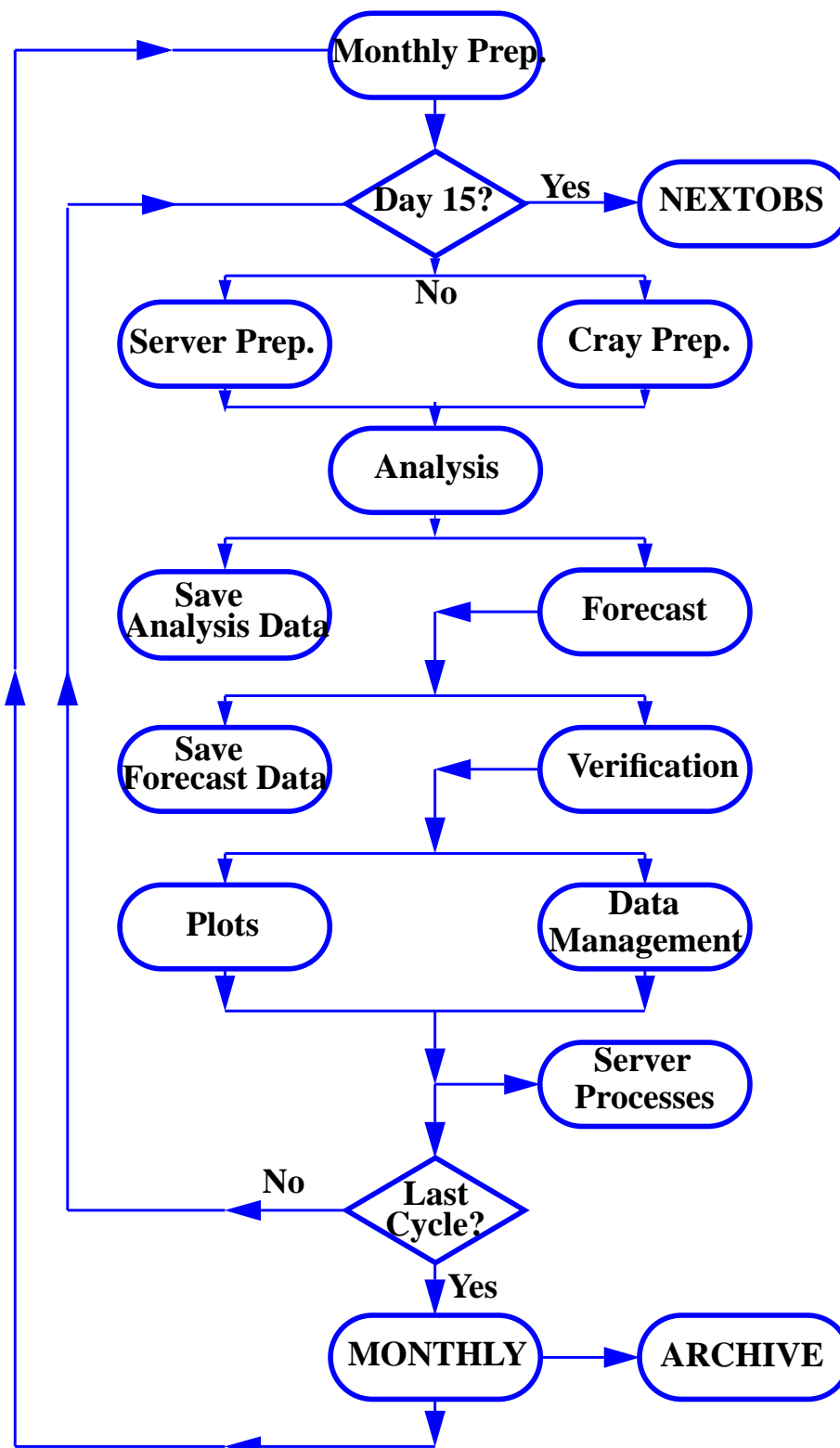


Figure 11 - The main components of the ERA system.

Results in the form of analysis and forecast fields were stored initially for a short time within the CRAY C90 fields data base, to allow rapid access by subsequent CRAY C90 tasks. They were also inserted into an EMPRESS data base on the SGI system soon after they had been produced, and accumulated for one month before being added to the IBM based archive. At all stages the fields data were accessible using MARS; thus the ERA system was fully re-startable from any data assimilation cycle within the month.

Analysis feedback statistics were moved to an SGI server as produced, and entered into an EMPRESS data base of identical structure to that used for the observations.

When the 15th of each month was reached the module to organize the observations for two months ahead was started; this enabled preparation of the observations to be completed well before they were needed, and action to be taken in good time when problems were detected.

At the end of each month of production the bias corrections required for the 1D-VAR system were computed from the accumulated statistics, and results for the current month added to the archive. Next, a search was made for the file containing the required information to generate the next month's blacklist of suspect stations. If this file existed, the blacklist was generated and the data assimilation module repeated for the next month. If not, the system suspended itself awaiting manual recovery.

Special dumps of strategic files, libraries and binaries were made at the end of each month of production; this enabled any month to be re-run, using starting conditions identical to those of the earlier production.

## **6.5 Adding results to the archive**

The ECMWF Meteorological Archive and Retrieval System (MARS) is the basic system for the management of the Centre's archives. MARS allows data to be described using a command language based on attributes which approximate to a reasonable meteorological definition of the data. Some of these attributes are universally obvious, such as parameter, level, time, step, and representation. Others are somewhat less intuitive, but enable a precise description to be made concerning which of a number of possible sub-sets of similar data are actually being defined. Thus attributes such as "expver" (experiment version number), and "class" (operational, research, ERA) provide full facilities for the extension of MARS not only for use with a project such as re-analysis, but also for the retention of many variants of the same data - especially useful where parts of a re-analysis may need to be re-run.

It was decided to archive ERA fields as monthly files within the MARS system. This allows efficient retrieval of long periods of data, and reduces the number of files to be accommodated. This is an important consideration, as the file management system on which MARS depends operates more efficiently if the numbers of files can be minimized. The MARS system provides the mapping between the described data (described in

Meteorological terms) and the physical data within physical files. It was also decided that all archive processes would be initiated from the SGI servers. To support this a considerable amount of development of the MARS system was required.

Within MARS a separate “class” has been added for ERA. This has enabled the MARS “expver” parameter to be used to distinguish between different versions of re-analysis data which have been added to the archive. It has also enabled checking and experimental runs to be made without prejudice to the main production archive.

In addition to the archive of the analysis and forecast fields, data sets containing important job output, selected post-script files, and files containing analysis feedback information are stored. An analysis of satellite data processing for each previous month was performed, resulting in appropriate plots and statistics which could be used carefully to monitor the performance of the 1D-Variational scheme. Tasks were also run at the end of each production month to compute radiosonde bias corrections for the next month.

## 6.6 Checking the archive files

It was essential to verify that the fields which had been added to the archive at the level of the IBM could be accessed. Since it would be too costly in terms of computer and disk space resources to retrieve and check every individual field, selected fields from at least two dates within every archive file were checked. The selected fields were retrieved, decoded, and summary information printed.

## 6.7 Production log

During the ERA production a considerable amount of monitoring was carried out in order to identify, and where possible rectify deficiencies. A production log was kept in which all changes and events of note were listed. Information concerning the use of satellite data, the various sources of observations, and the sea surface temperature used has already been given in section 3. on page 7. Table 5 lists those events noted during the production which may have a significant bearing on the re-analysis data.



**Table 5 - Events from the Production Log.**

| Year    | Date(s)                         | Event                                                                                                                                                                                                                                                                                                                      |
|---------|---------------------------------|----------------------------------------------------------------------------------------------------------------------------------------------------------------------------------------------------------------------------------------------------------------------------------------------------------------------------|
| 1979    | January 1979 to December 1981   | The vegetation field incorrectly contained the value 0% at all points on longitude 0.                                                                                                                                                                                                                                      |
| 1980    | September 1980 to December 1986 | “Desertification” in the re-analyses of the Western Amazon (Peru, Ecuador). It is believed that the OI analysis produces systematic pressure increments in one direction, leading to cooling in the lowest levels. Since relative humidity is analysed this leads to constant drying near the ground. (see also 6.8 below) |
| 1980    | 21 September                    | Reduced data in the 18:00 UTC analysis because of a data problem.                                                                                                                                                                                                                                                          |
| 1981-82 | Various                         | An ftp problem resulted in isolated GRIB fields within the archive being corrupt                                                                                                                                                                                                                                           |
| 1982    | 19 July                         | COADS removed from 12:00 UTC analysis because of a data problem.                                                                                                                                                                                                                                                           |
| 1982    | 10 August                       | Reduced data in 12:00 UTC analysis because of a data problem.                                                                                                                                                                                                                                                              |
| 1982    | 16 September                    | Reduced data in 18:00 UTC analysis because of a data problem.                                                                                                                                                                                                                                                              |
| 1982    | 18 September                    | Reduced data in 12:00 UTC analysis because of a data problem.                                                                                                                                                                                                                                                              |
| 1983    | December                        | First guess cloud water not fed into analysis (12:00 UTC on 23rd, 00:00 UTC on 24th, 06:00 UTC on 24th, 00:00 UTC on 27th, and 06:00 UTC on 31st)                                                                                                                                                                          |
| 1986    | December                        | Reduction in BUOY data over the Christmas period.                                                                                                                                                                                                                                                                          |
| 1987    | 1 January                       | The surface pressure of about 20 SYNOP stations in the Peru/Ecuador area were added to the blacklist to overcome the “desertification” problem.                                                                                                                                                                            |
| 1990    | 31 July                         | Reduction in TEMP and SYNOP data at 00:00 UTC.                                                                                                                                                                                                                                                                             |
| 1993    | 1 April to 29 April             | No PAOB data.                                                                                                                                                                                                                                                                                                              |

**Table 5 - Events from the Production Log.**

| Year       | Date(s) | Event                                                                                                                                                                                                                                                                                                                                                                                                                                                                                                                                                                                                                                                                                                                  |
|------------|---------|------------------------------------------------------------------------------------------------------------------------------------------------------------------------------------------------------------------------------------------------------------------------------------------------------------------------------------------------------------------------------------------------------------------------------------------------------------------------------------------------------------------------------------------------------------------------------------------------------------------------------------------------------------------------------------------------------------------------|
| Throughout |         | Due to a programming error in the forecast model, the entire ERA was run with very little regard to the latent heat of freezing/melting in the convection. The sensitivity of this error was evaluated in a one month parallel assimilation, and it was shown to impact the zonal mean temperature in the ITCZ to some extent, at most by 0.2K around 500mb. There was also a small impact on the precipitation, primarily as redistribution of local convective maxima in the ITCZ. Since the bug was only discovered after several years of assimilation, and was not considered too serious, it was decided to complete ERA with the bug included, in order not to introduce a discontinuity in the ITCZ 'climate'. |
| Throughout |         | For surface data the main source of observations were SYNOP reports exchanged over the WMO GTS. In the early years many stations did not report snow depth. Where available, the analysis system used takes account of reported snow depth. Thus in some areas the snow depth information within the re-analysis, especially for early years, is largely model generated.                                                                                                                                                                                                                                                                                                                                              |
| Throughout |         | Three "sea points" in Lake Victoria have constant sea surface temperatures of about 17 deg. C. which is too low. This results in a local minimum in convective precipitation over the lake.                                                                                                                                                                                                                                                                                                                                                                                                                                                                                                                            |
| Throughout |         | A spurious sea point within the Congo basin is seen to produce surface energy fluxes more typical of tropical ocean than neighbouring land points.                                                                                                                                                                                                                                                                                                                                                                                                                                                                                                                                                                     |

## 6.8 Post-production log

After finalizing the ERA-15 production, the output analysis and short-range forecast fields (listed in section 7.) have been used extensively and evaluated both internally at ECMWF and externally by the scientific community at large. During these activities some further problems and deficiencies have been uncovered. The most serious are listed here; more details about many of them may be found in Report No. 2 "Aspects of the Re-Analysed Climate" in this series of ECMWF Re-Analysis Project Reports.

- **Surface temperature in extremely stable conditions.** Primarily over the Antarctic Icesheet, but also noticed over Greenland, the ERA-15 surface temperatures drop to unrealistically low values, sometimes down to -90°C. In extremely stable conditions the vertical diffusion of heat in the forecast model vanished almost entirely. Hence the surface temperature was determined entirely by the radiative balance.

- **Antarctic orography.** The orography database used for ERA-15 had substantial errors in the interior of Antarctica, locally exceeding one kilometre.
- **Station height at Vostok.** The WMO reported station height of Vostok (107°E, 78.5°S) had an error of about 70 meters. This error was ‘too small’ to be discovered by the Quality Control procedures in the Optimum Interpolation (O/I) scheme in this otherwise completely data-void Antarctic interior. Hence there is a fictitious low in the mean ERA-15 analyses reaching from the surface at 600hPa a few 100hPa upwards. The mass and wind analyses should be used with utmost care in that part of the world.
- **Surface temperatures in boreal forests during spring.** An unrealistically large value was used for the albedo in high latitude regions covered by evergreen forests (taiga). As a consequence the ERA-15 surface and 2-metre temperatures are unrealistically cold in the affected areas during spring - still snow covered but with substantial solar radiation. Extremely, in parts of Siberia and Canada, the 2-metre temperature may be down to 10°C too cold in April. There is also some impact on temperatures in the lower free atmosphere, primarily below 850hPa.
- **Non-representative island stations.** In the O/I scheme, 10-metre winds from isolated island stations were used. Due to local effects, these observations are not representative of the near-surface wind fields over the surrounding sea. During the subsequent forecast phase of the data assimilation, the wind speeds in the vicinity of these stations recover, causing spin-up effects in the surface exchange processes. Primarily the evaporation and, consequently, the precipitation are affected, mostly in the ITCZ, and worst in the western Pacific.
- **The “Amazon” problem.** After several years of assimilation, a serious error was discovered in the soil temperatures and soil wetness in a small region in the western most equatorial Amazon basin (west of 70°W). From September 1980 to the end of 1986, this area is too hot and too dry. Due to the time limitations of the ERA project it was not possible to reprocess the full period affected once the problem was discovered. The period before September 1980 was, however, re-run for other reasons, and does contain the correction for this problem. The drying out was a combined effect of the O/I scheme using relative humidity as its humidity variable, and the local failure of the method used to compensate for the semi-diurnal tide in the observed surface pressures in this low lying area very close to the high Andes. After blacklisting surface pressure observations from the critical region, the soil and precipitation quickly recovered to realistic values, but the long term hydrology of the Amazon basin in ERA-15 is not correct. (see also table 5 in the previous section)
- **Temperature and humidity biases in the tropics.** In ERA-15 TOVS satellite cloud cleared radiances (CCRs) from a long series of NOAA satellites were used in a one-dimensional variational approach. The method requires a minimization of the effects of drift and sudden changes

in the instrumental outputs. This is done by inter-calibration and bias correction of the IR and microwave radiation from the radiometers. In spite of extensive monitoring, quality control and bias correction, the ERA-15 analyses suffer from changes in the instrument behaviour. The impact is seen as sudden 'jumps' in timeseries of the analyzed temperatures and humidities in the lower troposphere, primarily at low latitudes. The worst instance is in November 1986 when an unrealistically large scale warming and moistening of the ITCZ took place. Although these jumps are believed not to affect the day-to-day synoptic developments in ERA-15 too badly - they are for instance not noticeable in first guess comparisons with radiosondes - great care should nevertheless be taken when attempting to use the reanalyses for studies of, for example, long-term 'climate' trends.

## 7. Re-Analysis Output

### 7.1 Analysis and Forecast Fields

The WMO representation form FM92 GRIB is used to represent all analysis and forecast fields. In general, ERA GRIB data are coded using ECMWF's local version of GRIB code table 2 (version number 128), which gives parameter names and units. An additional local version of GRIB code table 2 (version 160) is used for some monthly, seasonal, yearly, and climatological parameters. Local version 160 was devised for ERA use, and enables time normalised flux values, variances, and co-variances to be represented. When allocating parameter numbers within table 160 a close correspondence with the numbering system of table 128 has been maintained. Thus, with a few minor exceptions, code figures from table 160 refer to the same parameters as code figures from table 128 (but with time normalised units for accumulated values). The exceptions are with respect to a few originally unused entries in table 128 used for extra parameters in table 160, which have since been allocated to serve other needs within table 128.

#### 7.1.1 Daily data

Primary data have been saved from each analysis, the four times daily 6 hour forecasts, and every six hourly intervals from the twice-daily forecasts extended to 24 hours. Initialised analysis data are stored as time 0 of the forecast data. Data from ten day forecasts based on ERA data have been saved at 12 hourly intervals throughout the forecasts. The resulting archive contains data at the resolution and on the spatial grid of the assimilation system for the 31 model levels (see *Vertical resolution: on page 30*), for 17 pressure levels (1000, 925, 850, 775, 700, 600, 500, 400, 300, 250, 200, 150, 100, 70, 50, 30, and 10 hPa), and for surface and single level parameters. In addition pressure level and single level data are available on a regular 2.5 degree latitude/longitude grid. Interpolation from T106 spherical harmonics has been achieved by first truncating to T47, then transforming to the 2.5 degree grid.

Table 6 gives details of the upper air parameters; these include the logarithm of surface pressure, which although not strictly an "upper air" parameter is produced in spherical harmonics along with the model level data, and is required to compute the pressures of the data points. The table indicates which parameters are stored at model levels, and which are stored on pressure levels. The various horizontal representations are indicated by sh (spherical harmonics), gg (Gaussian grid), and 2.5° (2.5 degree latitude/longitude grid). Except where indicated, parameters are available from both the analyses and the forecasts.

**Table 6 - Upper Air Parameters - daily archive**

| Parameter                  | model levels |                | pressure levels |                  | Code | Units                          |
|----------------------------|--------------|----------------|-----------------|------------------|------|--------------------------------|
|                            | lsh          | gg             | sh              | 2.5 <sup>o</sup> |      |                                |
| geopotential               | X            |                | X               | X                | 129  | m <sup>2</sup> s <sup>-2</sup> |
| temperature                | X            |                | X               | XX               | 130  | °K                             |
| u-velocity of wind         | X            |                |                 | X                | 131  | ms <sup>-1</sup>               |
| v-velocity of wind         | X            |                |                 | X                | 132  | ms <sup>-1</sup>               |
| specific humidity          |              | X              |                 | X <sup>a</sup>   | 133  | Kg/Kg                          |
| vertical velocity          | X            |                | X               | X                | 135  | Pa s <sup>-1</sup>             |
| vorticity                  | X            |                | X               |                  | 138  | s <sup>-1</sup>                |
| log surface pressure       | X            |                |                 |                  | 152  |                                |
| divergence                 | X            |                | X               |                  | 155  | s <sup>-1</sup>                |
| relative humidity          |              |                | X               | X                | 157  | %                              |
| cloud liquid water content |              | X <sup>b</sup> |                 |                  | 246  | Kg/Kg                          |
| cloud ice water content    |              | X <sup>b</sup> |                 |                  | 247  | Kg/Kg                          |
| cloud cover                |              | X <sup>b</sup> |                 |                  | 248  | (0-1)                          |

a. Note that the pressure level 2.5 degree specific humidity was generated using a formulation not consistent with that employed within the forecast model to convert between relative and specific humidity.

b. forecast only - not available from analysis.

A variety of surface and single level parameters are saved. The list of these differs according to whether they were produced by the analysis (an), the forecast after initialisation at time step 0 (Fc/0), or later steps within the forecast (Fc). Full details are given in Table 7 which also indicates, under “Code”, the GRIB code table 2 reference number given to each parameter.

Forecast accumulations of flux and precipitation data (Fa) have been extracted from the accumulation periods 12 to 18 hours, and 18 to 24 hours of the twice daily forecasts extended to 24 hours

**Table 7 - Surface and single level parameters - daily archive**

| Parameter                         | An | Fc/0 | Fc | Fa | Code | Units                          |
|-----------------------------------|----|------|----|----|------|--------------------------------|
| sea surface temperature           | X  |      |    |    | 11   | °K                             |
| ice cover (1 = ice, 0 = no ice)   | X  |      |    |    | 91   |                                |
| surface geopotential              | X  | X    |    |    | 129  | m <sup>2</sup> s <sup>-2</sup> |
| total column water <sup>a</sup>   |    | X    | X  |    | 136  | Kg/m <sup>2</sup>              |
| total column water vapour         |    | X    | X  |    | 137  | Kg/m <sup>2</sup>              |
| soil temperature level 1          | X  | X    | X  |    | 139  | °K                             |
| soil temperature level 2          | X  | X    | X  |    | 170  | °K                             |
| soil temperature level 3          | X  | X    | X  |    | 183  | °K                             |
| soil temperature level 4          | X  | X    | X  |    | 236  | °K                             |
| soil wetness level 1              | X  | X    | X  |    | 140  | m of water                     |
| soil wetness level 2              | X  | X    | X  |    | 171  | m of water                     |
| soil wetness level 3              | X  | X    | X  |    | 184  | m of water                     |
| soil wetness level 4              | X  | X    | X  |    | 237  | m of water                     |
| snow depth                        | X  | X    | X  | X  | 141  | m of water equivalent          |
| large scale precipitation         |    | X    | X  | X  | 142  | m of water                     |
| convective precipitation          |    | X    | X  | X  | 143  | m of water                     |
| snow fall                         |    | X    | X  | X  | 144  | m of water equivalent          |
| boundary layer dissipation        |    | X    | X  | X  | 145  | Wm <sup>-2</sup> s             |
| surface sensible heat flux        |    | X    | X  | X  | 146  | Wm <sup>-2</sup> s             |
| surface latent heat flux          |    | X    | X  | X  | 147  | Wm <sup>-2</sup> s             |
| mean sea level pressure           | X  | X    | X  |    | 151  | Pa                             |
| standard deviation of orography   | X  | X    |    |    | 160  |                                |
| anisotropy of orography           | X  | X    |    |    | 161  |                                |
| angle of sub-grid scale orography | X  | X    |    |    | 162  |                                |
| slope of sub-grid scale orography | X  | X    |    |    | 163  |                                |
| total cloud cover                 |    | X    | X  |    | 164  | (0-1)                          |
| 10 metre u-wind                   | X  | X    | X  |    | 165  | ms <sup>-1</sup>               |
| 10 metre v-wind                   | X  | X    | X  |    | 166  | ms <sup>-1</sup>               |

**Table 7 - Surface and single level parameters - daily archive**

| Parameter                                        | An | Fc/0 | Fc | Fa | Code | Units              |
|--------------------------------------------------|----|------|----|----|------|--------------------|
| 2 metre temperature                              | X  | X    | X  |    | 167  | °K                 |
| 2 metre dewpoint                                 | X  | X    | X  |    | 168  | °K                 |
| surface solar radiation downward <sup>b</sup>    |    |      | X  | X  | 169  | Wm <sup>-2</sup> s |
| land/sea mask                                    | X  | X    |    |    | 172  | (0,1)              |
| surface roughness                                | X  | X    |    |    | 173  | m                  |
| albedo                                           | X  | X    |    |    | 174  |                    |
| surface thermal radiation downwards <sup>b</sup> |    |      | X  | X  | 175  | Wm <sup>-2</sup> s |
| surface solar radiation                          |    |      | X  | X  | 176  | Wm <sup>-2</sup> s |
| surface thermal radiation                        |    |      | X  | X  | 177  | Wm <sup>-2</sup> s |
| top solar radiation                              |    |      | X  | X  | 178  | Wm <sup>-2</sup> s |
| top thermal radiation                            |    |      | X  | X  | 179  | Wm <sup>-2</sup> s |
| u-component of stress                            |    |      | X  | X  | 180  | Nm <sup>-2</sup> s |
| v-component of stress                            |    |      | X  | X  | 181  | Nm <sup>-2</sup> s |
| evaporation                                      |    |      | X  | X  | 182  | m of water         |
| convective cloud cover                           |    | X    | X  |    | 185  | (0-1)              |
| low cloud cover                                  |    | X    | X  |    | 186  | (0-1)              |
| medium cloud cover                               |    | X    | X  |    | 187  | (0-1)              |
| high cloud cover                                 |    | X    | X  |    | 188  | (0-1)              |
| latitudinal component of gravity wave stress     |    | X    | X  | X  | 195  | Nm <sup>-2</sup> s |
| meridional component of gravity wave stress      |    | X    | X  | X  | 196  | Nm <sup>-2</sup> s |
| gravity wave dissipation                         |    | X    | X  | X  | 197  | Wm <sup>-2</sup> s |
| skin reservoir content                           | X  | X    | X  |    | 198  | m of water         |
| percentage of vegetation                         | X  | X    |    |    | 199  | %                  |
| runoff                                           |    | X    | X  | X  | 205  | m of water         |
| instantaneous X component of surface stress      |    | X    | X  |    | 229  | Nm <sup>-2</sup>   |
| Instantaneous Y component of surface stress      |    | X    | X  |    | 230  | Nm <sup>-2</sup>   |
| instantaneous surface heat flux                  |    | X    | X  |    | 231  | Wm <sup>-2</sup>   |



**Table 7 - Surface and single level parameters - daily archive**

| Parameter                                       | An | Fc/0 | Fc | Fa | Code | Units                 |
|-------------------------------------------------|----|------|----|----|------|-----------------------|
| instantaneous moisture flux (evaporation)       |    | X    | X  |    | 232  | Kg/m <sup>2</sup> s   |
| apparent surface humidity                       | X  | X    | X  |    | 233  | Kg/Kg                 |
| log. surface roughness length for heat          | X  | X    |    |    | 234  |                       |
| skin temperature                                | X  | X    | X  |    | 235  | °K                    |
| convective snow fall                            |    |      | X  | X  | 239  | m of water equivalent |
| large scale snow fall                           |    |      | X  | X  | 240  | m of water equivalent |
| forecast albedo                                 |    |      | X  |    | 243  |                       |
| forecast surface roughness                      |    |      | X  |    | 244  | m                     |
| forecast log. surface roughness length for heat |    |      | X  |    | 245  |                       |

a. available December 1978 to August 1980, and March 1981 to February 1994 only.

b. available December 1978 to August 1980, and January 1983 to February 1994 only.

### 7.1.2 Monthly data

Monthly and seasonal averages, and a selection of variance and co-variance statistics have been computed for the 2.5 degree data, and for a selection of the full resolution data.

Where variables are listed under tables of monthly means they have been archived separately for each synoptic hour (00, 06, 12, and 18 UTC), and also as monthly “daily” means (monthly mean of the average of the four values for each day). Table 8 contains a list of upper air parameters for which monthly mean and monthly “daily” mean values have been added to the archive.

**Table 8 - Upper Air Parameters - monthly means and monthly “daily” means**

| Parameter                 | model levels |    | pressure levels |      | Code | Units                          |
|---------------------------|--------------|----|-----------------|------|------|--------------------------------|
|                           | sh           | gg | sh              | 2.5° |      |                                |
| Heaviside (beta) function |              |    |                 | X    | 254  | 0/1                            |
| geopotential              |              |    | X               | X    | 129  | m <sup>2</sup> s <sup>-2</sup> |
| temperature               | X            |    | X               | X    | 130  | °K                             |

**Table 8 - Upper Air Parameters - monthly means and monthly “daily” means**

| Parameter                  | model levels |                | pressure levels |                  | Code | Units              |
|----------------------------|--------------|----------------|-----------------|------------------|------|--------------------|
|                            | sh           | gg             | sh              | 2.5 <sup>o</sup> |      |                    |
| u-velocity of wind         |              |                |                 | X                | 131  | ms <sup>-1</sup>   |
| v-velocity of wind         |              |                |                 | X                | 132  | ms <sup>-1</sup>   |
| specific humidity          |              | X              |                 | X <sup>a</sup>   | 133  | Kg/Kg              |
| vertical velocity          | X            |                | X               | X                | 135  | Pa s <sup>-1</sup> |
| vorticity                  | X            |                | X               |                  | 138  | s <sup>-1</sup>    |
| divergence                 | X            |                | X               |                  | 155  | s <sup>-1</sup>    |
| relative humidity          |              |                | X               | X                | 157  | %                  |
| cloud liquid water content |              | X <sup>b</sup> |                 |                  | 246  | Kg/Kg              |
| cloud ice water content    |              | X <sup>a</sup> |                 |                  | 247  | Kg/Kg              |
| cloud cover                |              | X <sup>a</sup> |                 |                  | 248  | (0-1)              |

a. Note that the pressure level 2.5 degree specific humidity was generated using a formulation not consistent with that employed within the forecast model to convert between relative and specific humidity.

b. forecast only - not available from analysis.

Mean and variance values for the 2.5 degree pressure level data have been computed in two ways. First, simple means and variances were produced without regard to the value of the pressure level concerned with respect to the surface pressure. Secondly, values were re-computed using the “Heaviside” step function

$$\beta = \begin{cases} 1, & P < P_s \\ 0, & P \geq P_s \end{cases}$$

A list of variance and co-variance data added to the archive is contained in Table 9 below.

**Table 9 - Upper Air Parameters - variance and co-variance data**

| Parameter          | Code | Units                          |
|--------------------|------|--------------------------------|
| geopotential       | 129  | m <sup>2</sup> s <sup>-2</sup> |
| temperature        | 130  | °K                             |
| u-velocity of wind | 131  | ms <sup>-1</sup>               |
| v-velocity of wind | 132  | ms <sup>-1</sup>               |
| specific humidity  | 133  | Kg/Kg                          |

**Table 9 - Upper Air Parameters - variance and co-variance dats**

| Parameter                                    | Code | Units                            |
|----------------------------------------------|------|----------------------------------|
| vertical velocity                            | 135  | Pa s <sup>-1</sup>               |
| relative humidity                            | 157  | %                                |
| SD of geopotential                           | 206  | m <sup>2</sup> s <sup>-2</sup>   |
| cov. temperature and geopotential            | 207  | Km <sup>2</sup> s <sup>-2</sup>  |
| SD of temperature                            | 208  | K                                |
| cov. sp. humidity and geopotential           | 209  | m <sup>2</sup> s <sup>-2</sup>   |
| cov. sp. humidity and temperature            | 210  | K                                |
| SD of specific humidity                      | 211  | (0 - 1)                          |
| cov. u-wind and geopotential                 | 212  | m <sup>3</sup> s <sup>-3</sup>   |
| cov. u-wind and temperature                  | 213  | Kms <sup>-1</sup>                |
| cov. u-wind and specific humidity            | 214  | ms <sup>-1</sup>                 |
| SD of u-velocity of wind                     | 215  | ms <sup>-1</sup>                 |
| cov. v-wind and geopotential                 | 216  | m <sup>3</sup> s <sup>-3</sup>   |
| cov. v-wind and temperature                  | 217  | Kms <sup>-1</sup>                |
| cov. v-wind and specific humidity            | 218  | ms <sup>-1</sup>                 |
| cov. v-wind and u-wind                       | 219  | m <sup>2</sup> s <sup>-2</sup>   |
| SD of v-velocity of wind                     | 220  | ms <sup>-1</sup>                 |
| cov. vertical velocity and geopotential      | 221  | Pam <sup>2</sup> s <sup>-3</sup> |
| cov. vertical velocity and temperature       | 222  | KPas <sup>-1</sup>               |
| cov. vertical velocity and specific humidity | 223  | Pas <sup>-1</sup>                |
| cov. vertical velocity u-wind                | 224  | Pams <sup>-2</sup>               |
| cov. vertical velocity and v-wind            | 225  | Pams <sup>-2</sup>               |
| SD of vertical velocity                      | 226  | Pas <sup>-1</sup>                |
| SD of relative humidity                      | 227  | %                                |

For surface and single level parameters monthly values were created both for each model produced parameter on an “as is” basis, and in a time normalised manner.

In the “as is” set flux values are accumulated from the beginning of each forecast, resulting in 6, 12, 18, and 24 hour accumulations from 6, 12, 18, and 24 hour forecasts respectively. Monthly mean, monthly mean of daily means, and monthly variance data were generated for each parameter. Table 10 lists the parameters saved into the archive from this set.

**Table 10 - Surface and single level parameters - monthly archive**

| Parameter                                     | An | Fc/0 | Fc | Code | Units                 |
|-----------------------------------------------|----|------|----|------|-----------------------|
| total column water <sup>a</sup>               |    | X    | X  | 136  | Kg/m <sup>2</sup>     |
| total column water vapour                     |    | X    | X  | 137  | Kg/m <sup>2</sup>     |
| soil temperature level 1                      | X  | X    | X  | 139  | °K                    |
| soil temperature level 2                      | X  | X    | X  | 170  | °K                    |
| soil temperature level 3                      | X  | X    | X  | 183  | °K                    |
| soil temperature level 4                      | X  | X    | X  | 236  | °K                    |
| soil wetness level 1                          | X  | X    | X  | 140  | m of water            |
| soil wetness level 2                          | X  | X    | X  | 171  | m of water            |
| soil wetness level 3                          | X  | X    | X  | 184  | m of water            |
| soil wetness level 4                          | X  | X    | X  | 237  | m of water            |
| snow depth                                    | X  | X    | X  | 141  | m of water equivalent |
| large scale precipitation                     |    |      | X  | 142  | m of water            |
| convective precipitation                      |    |      | X  | 143  | m of water            |
| snow fall                                     |    |      | X  | 144  | m of water equivalent |
| boundary layer dissipation                    |    |      | X  | 145  | Wm <sup>-2</sup> s    |
| surface sensible heat flux                    |    |      | X  | 146  | Wm <sup>-2</sup> s    |
| surface latent heat flux                      |    |      | X  | 147  | Wm <sup>-2</sup> s    |
| mean sea level pressure                       | X  | X    | X  | 151  | Pa                    |
| total cloud cover                             |    | X    | X  | 164  | (0-1)                 |
| 10 metre u-wind                               | X  | X    | X  | 165  | ms <sup>-1</sup>      |
| 10 metre v-wind                               | X  | X    | X  | 166  | ms <sup>-1</sup>      |
| 2 metre temperature                           | X  | X    | X  | 167  | °K                    |
| 2 metre dewpoint                              | X  | X    | X  | 168  | °K                    |
| surface solar radiation downward <sup>b</sup> |    |      | X  | 169  | Wm <sup>-2</sup> s    |

**Table 10 - Surface and single level parameters - monthly archive**

| Parameter                                        | An | Fc/0 | Fc | Code | Units                 |
|--------------------------------------------------|----|------|----|------|-----------------------|
| surface thermal radiation downwards <sup>b</sup> |    |      | X  | 175  | Wm <sup>-2</sup> s    |
| surface solar radiation                          |    |      | X  | 176  | Wm <sup>-2</sup> s    |
| surface thermal radiation                        |    |      | X  | 177  | Wm <sup>-2</sup> s    |
| top solar radiation                              |    |      | X  | 178  | Wm <sup>-2</sup> s    |
| top thermal radiation                            |    |      | X  | 179  | Wm <sup>-2</sup> s    |
| u-component of stress                            |    |      | X  | 180  | Nm <sup>-2</sup> s    |
| v-component of stress                            |    |      | X  | 181  | Nm <sup>-2</sup> s    |
| evaporation                                      |    |      | X  | 182  | m of water            |
| low cloud cover                                  |    | X    | X  | 186  | (0-1)                 |
| medium cloud cover                               |    | X    | X  | 187  | (0-1)                 |
| high cloud cover                                 |    | X    | X  | 188  | (0-1)                 |
| latitudinal component of gravity wave stress     |    | X    | X  | 195  | Nm <sup>-2</sup> s    |
| meridional component of gravity wave stress      |    | X    | X  | 196  | Nm <sup>-2</sup> s    |
| gravity wave dissipation                         |    | X    | X  | 197  | Wm <sup>-2</sup> s    |
| skin reservoir content                           | X  | X    | X  | 198  | m of water            |
| runoff                                           |    | X    | X  | 205  | m of water            |
| skin temperature                                 | X  | X    | X  | 235  | °K                    |
| convective snow fall                             |    |      | X  | 239  | m of water equivalent |
| large scale snow fall                            |    |      | X  | 240  | m of water equivalent |
| 10m wind speed (irrespective of direction)       | X  | X    | X  | 246  | ms <sup>-1</sup>      |
| momentum flux (irrespective of direction)        |    |      | X  | 247  | Nm <sup>-2</sup>      |

a. available December 1978 to August 1980, and March 1981 to February 1994 only.

b. available December 1978 to August 1980, and January 1983 to February 1994 only.

Additionally forecast accumulations of flux and precipitation parameters were generated in time normalised form both from the 6 hour “first guess” forecasts, and from the period 12 to 24 hours of the twice daily 24 hour forecasts, giving monthly means for specific hours (Fa/mo), and monthly means of daily averages (Fa/

moda). Note that GRIB code table 2 version 160 is used for this set, reflecting the time normalised units.

Table 11 lists the archived parameters.

**Table 11 - Forecast accumulations - monthly mean data**

| Parameter                                        | Fa/mo | Fa/moda | Code | Units                          |
|--------------------------------------------------|-------|---------|------|--------------------------------|
| large scale precipitation                        | X     | X       | 142  | $\text{kgm}^{-2}\text{s}^{-1}$ |
| convective precipitation                         | X     | X       | 143  | $\text{kgm}^{-2}\text{s}^{-1}$ |
| snow fall                                        | X     | X       | 144  | $\text{kgm}^{-2}\text{s}^{-1}$ |
| boundary layer dissipation                       | X     | X       | 145  | $\text{Wm}^{-2}$               |
| surface sensible heat flux                       | X     | X       | 146  | $\text{Wm}^{-2}$               |
| surface latent heat flux                         | X     | X       | 147  | $\text{Wm}^{-2}$               |
| surface solar radiation downward <sup>a</sup>    | X     | X       | 169  | $\text{Wm}^{-2}$               |
| surface thermal radiation downwards <sup>a</sup> | X     | X       | 175  | $\text{Wm}^{-2}$               |
| surface solar radiation                          | X     | X       | 176  | $\text{Wm}^{-2}$               |
| surface thermal radiation                        | X     | X       | 177  | $\text{Wm}^{-2}$               |
| top solar radiation                              | X     | X       | 178  | $\text{Wm}^{-2}$               |
| top thermal radiation                            | X     | X       | 179  | $\text{Wm}^{-2}$               |
| u-component of stress                            |       | X       | 180  | $\text{Nm}^{-2}$               |
| v-component of stress                            |       | X       | 181  | $\text{Nm}^{-2}$               |
| evaporation                                      |       | X       | 182  | $\text{kgm}^{-2}\text{s}^{-1}$ |
| latitudinal component of gravity wave stress     | X     | X       | 195  | $\text{Nm}^{-2}$               |
| meridional component of gravity wave stress      | X     | X       | 196  | $\text{Nm}^{-2}$               |
| gravity wave dissipation                         | X     | X       | 197  | $\text{Wm}^{-2}$               |
| runoff                                           | X     | X       | 205  | $\text{kgm}^{-2}\text{s}^{-1}$ |
| convective snow fall                             | X     | X       | 239  | $\text{kgm}^{-2}\text{s}^{-1}$ |
| large scale snow fall                            | X     | X       | 240  | $\text{kgm}^{-2}\text{s}^{-1}$ |
| momentum flux                                    | X     | X       | 247  | $\text{Nm}^{-2}$               |

a. available December 1978 to August 1980, and January 1983 to February 1994 only.

## 7.2 Data from ERA - observations and feedback

The observed values presented to the analyses together with difference statistics with respect to the analyses, the initialized analyses, and the 6 hour forecasts used as “first guess” have been stored. The difference statistics contained within these data contain a wealth of information concerning the characteristics of the data assimilation system, and of the observing system.

## 7.3 Other data

Throughout the ERA production all important job output for the various sub-systems of the production system were collected into monthly files and added to the archives. Individual outputs for single jobs within these files can be obtained where required, enabling investigations to be carried out into specific cases where necessary.

As routine, a number of graphical plots were generated and stored on-line for monitoring purposes. These include data coverage maps, analysis increments, and maps of selected parameters. At the end of each production month these plot files were organised into a suitable form and added to the archive.

## 7.4 Availability of ERA data

Data from ERA are made available to research scientists throughout the world. The Data Services Unit at ECMWF are able to extract and supply sub-sets of data to meet users' requirements, and will supply full details on request. Enquiries should be addressed to:

Data Services,  
ECMWF,  
Shinfield Park,  
Reading, RG2 9AX,  
U.K.

or by e-mail to [data.services@ecmwf.int](mailto:data.services@ecmwf.int).

Additionally, selected data are available to the German academic community from the Max-Planck-Institut, Hamburg; to the United Kingdom academic community through the British Atmospheric Data Centre, Rutherford Appleton Laboratory, Didcot; to the UCAR community in the United States of America through the National Center for Atmospheric Research; and to the Atmospheric Model Intercomparison Project (AMIP) community through the Program for Climate Model Diagnostics and Intercomparison (PCMDI), University of California, Lawrence Livermore National Laboratory.

## 8. Concluding Remarks

The production of a completely consistent global re-analysis would require a consistent observing system with respect both to the quantity and quality of observations. This requirement cannot be met in its entirety from the historical record. In consequence, the ERA project has attempted to apply a consistent data assimilation scheme to a reasonable sub-set of those data which are available, and to contributing components of the observing system which have been reasonably consistent throughout the 15 year period.

Probably the most important contributing system is the cloud cleared radiance data set from the polar orbiting satellites. Through the use of the 1D-Variational method a specific attempt has been made within the ERA project to maximise the use of these data with respect both to the mass/wind analyses and the humidity analyses.

The very considerable efforts made initially to ensure the selection of a suitably high quality assimilation system led to a programme of research and experimentation which yielded much in terms of useful feedback and development not only for ERA but also for ECMWF's research and operations.

Data from ERA are already extensively used for research purposes within ECMWF, and have provided the raw material for a number of interesting validation reports (ECMWF, 1997). They have been made available to the ECMWF Member States through the Centre's archives, to the AMIP community through PCMDI, to the United States' academic community through UCAR/NCAR, and to research workers elsewhere through the ECMWF Data Services.



## References:

- Andersson, E., Hollingsworth, A., Kelly, G., Lonnberg, P., Pailleux, J. and Zhang, Z. 1991: Global observing system experiments on operational statistical retrievals of satellite sounding data. *Mon. Weather Rev.*, 119, 1851-1864.
- Bengtsson, L., Shukla, J., 1988: Integration of Space and In Situ Observations to Study Global Climate Change. *Bull. Amer. Meteorol. Soc.*, 69, 1130-1143.
- ECMWF Data Assimilation, 1992: Research Manual 1 - ECMWF Data Assimilation Scheme - Scientific Documentation - ECMWF Meteorol. Bull. M1.5/3.
- ECMWF Forecast System, 1992: Research Manual 2 - ECMWF Forecast Model Documentation - Adiabatic Part - ECMWF Meteorol. Bull. M1.6/3.
- ECMWF Forecast System, 1992: Research Manual 3 - ECMWF Forecast Model Documentation - Physical Parametrization - ECMWF Meteorol. Bull. M1.6/2.
- Eliassen, A., 1954: Provisional report on calculation of spatial covariance and autocorrelation of the pressure field. *Inst. Weather and Climate Res., Acad. Sci. Oslo, Rept. No. 5.*
- Eyre, J. R. 1989: Inversion of cloudy satellite sounding radiances by nonlinear optimal estimation. *Q. J. R. Meteorol. Soc.*, 113, 1001-1037.
- Eyre, J. R. 1991: A fast radiative transfer model for satellite sounding systems. *ECMWF Technical Memorandum 176.*
- Eyre, J. R. 1992: A bias correction scheme for simulated TOVS brightness temperatures. *ECMWF Technical Memorandum 186.*
- Eyre, J. R., Kelly, G. A., McNally, A. P., and Anderson, E., 1992: Assimilation of TOVS radiance information through one-dimensional variational analysis - *ECMWF Technical Memorandum No. 187, July 1992.*
- Eyre, J. R., Kelly, G. A., McNally, A. P., Andersson, E. and Persson, A. 1993: Assimilation of TOVS radiance information through one-dimensional variational analysis. *Q. J. R. Meteorol. Soc.*, 119, 1427-1463.
- Gandin, L. S., 1963: Objective analysis of meteorological fields. Translated from Russian by Israeli Program of Scientific Translations, 1965, 242pp.

- Jakob, C., 1994: The Impact of the New Cloud Scheme on ECMWF's Integrated Forecast System (IFS). Proceedings of ECMWF/GEWEX Workshop on Modelling, Validation and Assimilation of Clouds, ECMWF, November 1994.
- Lönnberg P., 1988: Developments in the ECMWF analysis system. ECMWF Seminar Proceedings - Data assimilation and the use of satellite data. Vol. I, 75-119.
- Lorenc A.C., 1981: A global three-dimensional multivariate statistical interpretation scheme. *Mon. Weather Rev.*, 109, 701-721.
- Lott, F., and Miller, M. J., 1997: A new subgrid-scale orographic drag parametrization: Its formulation and testing. *Quart. J. Roy. Meteor. Society*, 123, 101-127.
- Mahfouf, J.F., 1991: Analysis of soil moisture from near surface parameters: A feasibility study. *J. Appl. Meteor.*, 30, 1534-1547.
- McMillin, L. M., and Dean, C. 1982: Evaluation of a new operational technique for producing clear radiances. *J. Appl. Meteorol.*, 21, 1005-1014.
- McNally, A. P., and Vesperini, M., 1996: Variational analysis of humidity information from TOVS radiances. *Q. J. R. Meteorol. Soc.*, 122, 1521-1544.
- NESDIS, 1993: Polar Orbiter Archived TOVS Soundin Data Change and Problem Record, and TOVS Operational Processing/Changes. NOAA/NESDIS, personal communication.
- Nomura A., 1997: Global Sea Ice Concentration Data Set for use with the ECMWF Re-Analysis System ECMWF Project Report Series, 4. (previously issued as ECMWF Technical Report No. 76, March 1995.)
- NSIDC, 1992: DMSP SSM/I Brightness Temperature and Sea Ice Concentration Grids for the Polar Regions on CD-ROM. User's Guide.
- NSIDC, 1993: Nimbus-7 SMMR Polar Radiances and Arctic and Antarctic Sea Ice Concentrations on CD-ROM. User's Guide, Third Revised Edition.
- Gaffen, D. J., 1993: WMO TD No. 541.
- Parker, D. E., Folland C. K., Ward M. N., Jackson M., and Maskell K., 1995: Marine surface data for analysis of climate fluctuations on interannual to century timescales. In D. G. Martinson, K. Bryan, M. Ghil, M. M. Hall, T. R. Karl, E. S. Sarachik, S. Sorooshian, and L. D. Talley, editors, *Natural Cli-*

- mate Variability on Decade-to-Century Time Scales, 241-250. National Academy Press, Washington, D.C.
- Pesonen, O., and Raoult, B., 1992: SMS and CDP User Guide and Reference Manual, ECMWF.
- Rayner, N. A., Horton E. B., Parker D. E., Folland C. K., and Hackett R. B., 1996: Version 2.2 of the Global sea-ice and Sea Surface Temperature data set, 1903-1994. CRTN 74, September 1996, Hadley Centre.
- Reynolds, R. W. and Smith T. M., 1994: Improved Global Sea Surface Temperature Analysis Using Optimum Interpolation. *J. Climate*, 7, 929-948.
- Ritchie H., Temperton C., Simmons A.J., Hortal M., Davies T., Dent D., Hamrud M., 1995: Implementation of the Semi-Lagrangian Method in a High Resolution Version of the ECMWF Forecast Model. *Mon. Weather Rev.*, 123, 489-514.
- Shaw D.B., Lönnberg P., Hollingsworth A. and Undén P., 1987: Data assimilation: The 1984/85 revision of the ECMWF mass and wind analysis. *Q. J. R. Meteorol. Soc.*, 113, 533-566.
- Slingo J.J., 1987: The development and verification of a cloud prediction scheme for the ECMWF model. *Q. J. R. Meteorol. Soc.*, 213, 899-927.
- Smith, W. L., Woolf, H. M., 1976: The use of eigenvectors of statistical covariance matrices for interpreting satellite sounding radiometer observations. *J. Atmos. Sci.*, 33, 1127-1150.
- Tiedtke M., 1989: A comprehensive massflux scheme for cumulus parametrization in large-scale models. *Mon. Weather Rev.*, 117, 1779-1800.
- Tiedtke M, 1993: Representation of clouds in large-scale models. *Mon. Weather Rev.*, 121, 3040-3061
- Undén P., 1989: Tropical data assimilation and analysis of divergence. *Mon. Weather Rev.*, 117, 2495-2517.
- Vasiljevic, D., 1990; Use of First Guess at Appropriate Time. ECMWF Research Departments Memorandum R2327/2591.
- Viterbo, P., and Beljaars, A.C.M., 1995: An improved land surface parametrization scheme in the ECMWF model and its validation. *J. Clim.*, 8, 2716-2748.
- Viterbo, P., and Courtier, P., 1995: The importance of soil water for medium-range weather forecasting. Implications for data assimilation. International workshop of slowly varying components of pre-

dictable atmospheric motions, Beijing, China, 7-10 March 1995. PWPR Rep. Ser. No. 6, WMO/TD No. 652, 121-130.

Viterbo, P., 1996: The representation of surface processes in general circulation models. Doctorial thesis, ECMWF, 1-201.

Wallace J. M, Tibaldi S.,and Simmons A. J., 1983: Reduction of systematic forecast errors in the ECMWF model through the introduction of an envelope orography. *Q. J. R. Meteorol. Soc.*, 109, 683-717.

Woodruff, S.D., Lubker, S.J., Wolter, K., Worley, S.J., and Elms, J.D., 1993: Comprehensive Ocean-Atmosphere Data Set (COADS) Release 1a.: 1980-92. *Earth System Monitor*, 4, No. 1, 1-8.

## Bibliography:

### *ECMWF Re-Analysis Project Report Series*

ECMWF, 1997: ECMWF Re-Analysis Validation Reports - Part 2. ECMWF Re-Analysis Project Report Series, 7 onwards, in preparation.

Gibson, J.K., Kållberg, P., Uppala, S., Nomura, A., Hernandez, A., Serrano, E., 1997: ERA Description. ECMWF Re-Analysis Project Report Series, 1.

Kållberg, P., 1997: Aspects of the Re-Analysed Climate. ECMWF Re-Analysis Project Report Series, 2.

Nomura A., 1997: Global Sea Ice Concentration Data Set for use with the ECMWF Re-Analysis System ECMWF Project Report Series, 4. (previously issued as ECMWF Technical Report No. 76, March 1995.)

Serrano, E., 1997: Tropical Cyclones. ECMWF Re-Analysis Project Report Series, 5.

Stendel, M., and Arpe, K., 1997: Evaluation of the Hydrological Cycle in Re-Analysis and Observations. ECMWF Re-Analysis Validation Reports - Part 1. ECMWF Re-Analysis Project Report Series, 6.

Uppala, S., 1997: Observing System Performance in ERA. ECMWF Re-Analysis Project Report Series, 3.

### *ECMWF Re-Analysis data sources and forcing fields*

Gaffen, D. J., 1993: WMO TD No. 541.

Nomura A., 1995: Global Sea Ice Concentration Data Set for use with the ECMWF Re-Analysis System. ECMWF Technical Report No. 76, March 1995.

NSIDC, 1992: DMSP SSM/I Brightness Temperature and Sea Ice Concentration Grids for the Polar Regions on CD-ROM. User's Guide.

NSIDC, 1993: Nimbus-7 SMMR Polar Radiances and Arctic and Antarctic Sea Ice Concentrations on CD-ROM. User's Guide, Third Revised Edition.

Parker, D. E., Folland C. K., Ward M. N., Jackson M., and Maskell K., 1995: Marine surface data for analysis of climate fluctuations on interannual to century timescales. In D. G. Martinson, K. Bryan, M. Ghil, M. M. Hall, T. R. Karl, E. S. Sarachik, S. Sorooshian, and L. D. Talley, editors, Natural Cli-

mate Variability on Decade-to-Century Time Scales, 241-250. National Academy Press, Washington, D.C.

Rayner, N. A., Horton E. B., Parker D. E., Folland C. K., and Hackett R. B., 1996: Version 2.2 of the Global sea-ice and Sea Surface Temperature data set, 1903-1994. CRTN 74, September 1996, Hadley Centre.

Reynolds, R. W. and Smith T. M., 1994: Improved Global Sea Surface Temperature Analysis Using Optimum Interpolation. *J. Climate*, 7, 929-948.

Woodruff, S.D., Lubker, S.J., Wolter, K., Worley, S.J., and Elms, J.D., 1993: Comprehensive Ocean-Atmosphere Data Set (COADS) Release 1a.: 1980-92. *Earth System Monitor*, 4, No. 1, 1-8.

### ***ECMWF Re-Analysis miscellaneous references***

Boer, G.J, 1982. Diagnostic Equations in Isobaric Coordinates. *Mon. Weather Rev.*, 110, 1801-1820.

Källberg, P., and DelSol, F., 1986: Systematic Biases in Cloud-Track-Wind Data from Jet-Stream Regions. in "Collection of Papers Presented at the WMO/IUGG Symposium, Tokyo, 4-8 August 1986", Special Volume of the *J. Meteorol. Soc. of Japan*, 91-106.

Pesonen, O., and Raoult, B., 1992: SMS and CDP User Guide and Reference Manual, ECMWF.

Randel, David L., Vonder Haar, T. H., Ringerud, M. A., Stephens, G. L., Greenwald, T. J., and Combs, C. L., 1996: A new global water vapor dataset. *Bull. Amer. Meteorol. Soc.*, 77, No.6 1233-1246

Uppala, S., 1996: Observational statistics on the performance of the ECMWF Re-Analysis system during the period 1979-1983. Seventh Symposium on Global Change Studies, *Amer. Meteorol. Soc.*, 116-119.

### ***Satellite data one dimensional variational system***

Andersson, E., Hollingsworth, A., Kelly, G., Lonnberg, P., Pailleux, J. and Zhang, Z. 1991: Global observing system experiments on operational statistical retrievals of satellite sounding data. *Mon. Weather Rev.*, 119, 1851-1864.

Eyre, J. R. 1989: Inversion of cloudy satellite sounding radiances by nonlinear optimal estimation. *Q. J. R. Meteorol. Soc.*, 113, 1001-1037.

- Eyre, J. R. 1991: A fast radiative transfer model for satellite sounding systems. ECMWF Technical Memorandum 176.
- Eyre, J. R. 1992: A bias correction scheme for simulated TOVS brightness temperatures. ECMWF Technical Memorandum 186.
- Eyre, J. R., Kelly, G. A., McNally, A. P., and Anderson, E., 1992: Assimilation of TOVS radiance information through one-dimensional variational analysis - ECMWF Technical Memorandum No. 187, July 1992.
- Eyre, J. R., Kelly, G. A., McNally, A. P., Andersson, E. and Persson, A. 1993: Assimilation of TOVS radiance information through one-dimensional variational analysis. Q. J. R. Meteorol. Soc., 119, 1427-1463.
- ITPP-5.0 User Guide, 1995 Cooperative Institute for Meteorological Satellite Studies (CIMSS), University of Wisconsin-Madison..
- McMillin, L. M., and Dean, C. 1982: Evaluation of a new operational technique for producing clear radiances. J. Appl. Meteorol., 21, 1005-1014.
- McNally, A. P., and Vesperini, M., 1996: Variational analysis of humidity information from TOVS radiances. Q. J. R. Meteorol. Soc., 122, 1521-1544.
- NESDIS, 1993: Polar Orbiter Archived TOVS Soundin Data Change and Problem Record, and TOVS Operational Processing/Changes. NOAA/NESDIS, personal communication.
- Smith, W. L., Woolf, H. M., 1976: The use of eigenvectors of statistical covariance matrices for interpreting satellite sounding radiometer observations. J. Atmos. Sci., 33, 1127-1150.
- Smith, W. L., Woolf, H. M., Hayden, C. M., Wark, D. Q. and McMillin, L. M. 1979: The TIROS-N Operational Vertical Sounder. Bull. Amer. Meteorol. Soc., 60, 1177-1187.

### *Analysis system*

- Bengtsson L., Kanamitsu M., Kallberg P. and Uppala. S., 1982: FGGE 4-dimensional data assimilation at ECMWF. Bull. Amer. Meteorol. Soc., 63, 29-43.
- Bengtsson, L., Shukla, J., 1988: Integration of Space and In Situ Observations to Study Global Climate Change. Bull. Amer. Meteorol. Soc., 69, 1130-1143.

- ECMWF Data Assimilation, 1992: Research Manual 1 - ECMWF Data Assimilation Scheme - Scientific Documentation - ECMWF Meteorol. Bull. M1.5/3.
- Eliassen, A., 1954: Provisional report on calculation of spatial covariance and autocorrelation of the pressure field. Inst. Weather and Climate Res., Acad. Sci. Oslo, Rept. No. 5.
- Gandin, L. S., 1963: Objective analysis of meteorological fields. Translated from Russian by Israeli Program of Scientific Translations, 1965, 242pp.
- Hollingsworth A., Lönnberg P., 1986: The statistical structure of short-range forecast errors as determined from radiosonde data. Part I: The wind field. *Tellus*, 38A, 111-136.
- Hollingsworth A., Shaw D.B., Lönnberg P., Illari L., Arpe K. and Simmons A.J., 1986: Monitoring of observation and analysis quality by a data assimilation system. *Mon. Weather Rev.*, 114, 5, 861-879.
- Lönnberg P., Hollingsworth A., 1986: The statistical structure of short-range forecast errors as determined from radiosonde data. Part II: The covariance of heights and wind errors, *Tellus* 38A, 137-161.
- Lönnberg P., 1988: Developments in the ECMWF analysis system. ECMWF Seminar Proceedings - Data assimilation and the use of satellite data. Vol. I, 75-119.
- Lorenc A.C., 1981: A global three-dimensional multivariate statistical interpretation scheme. *Mon. Weather Rev.*, 109, 701-721.
- Schmetz, J., 1991 Further improvements of Cloud Motion Wind extraction techniques. Proceedings, Workshop on wind extraction from operational meteorological satellite data, Washington, D. C., EUMETSAT, NOAA and WMO.
- Shaw D.B., Lönnberg P., Hollingsworth A. and Undén P., 1987: Data assimilation: The 1984/85 revision of the ECMWF mass and wind analysis. *Q. J. R. Meteorol. Soc.*, 113, 533-566.
- Undén P., 1989: Tropical data assimilation and analysis of divergence. *Mon. Weather Rev.*, 117, 2495-2517.
- Vasiljevic, D., 1990; Use of First Guess at Appropriate Time. ECMWF Research Departments Memorandum R2327/2591.

### ***Normal Mode Initialisation***

- Machenhauer B., 1977: On the dynamics of gravity oscillations in a shallow water model, with application to normal mode initialization. *Beitr. Physics Atmos.* 50, 259-271.



Temperton C., Williamson D.L., 1981: Normal mode initialisation for a multivariate grid-point model: Part I linear aspects. *Mon. Weather Rev.*, 109, 720;743.

Temperton C., 1988: Implicit normal mode initialization. *Mon. Weather Rev.*, 116, 1013-1031.

Wergen W., 1988: The diabatic ECMWF normal mode initialisation scheme. *Beitr. Physics Atmosph.* 61, 274-304.

Williamson D.L., Temperton C., 1981: Normal mode initialisation for a multivariate grid-point model: Part II nonlinear aspects. *Mon. Weather Rev.*, 109, 744-757.

### *Prediction model*

ECMWF Forecast System, 1992: Research Manual 2 - ECMWF Forecast Model Documentation - Adiabatic Part - ECMWF Meteorol. Bull. M1.6/3.

ECMWF Forecast System, 1992: Research Manual 3 - ECMWF Forecast Model Documentation - Physical Parametrization - ECMWF Meteorol. Bull. M1.6/2.

Geleyn J.F., Hollingsworth A., 1979: An economical analytical method for the computation of the interaction between scattering and line absorption of radiation. *Beitr. Phys. Atmos.*, 52, 1-16.

Geleyn J.F., Preuss H.J., 1983: A new data set of satellite-derived surface albedo values for operational use at ECMWF. *Arch. Meteorol. GeoPhysics Bioclim., Ser. A*, 32, 353-359.

Geleyn J.F., 1988: Interpolation of wind temperature and humidity values from model levels to the height of measurements. *Tellus*, 40A, 347-351.

Hortal M., Simmons A., 1991: Use of reduced Gaussian grids in spectral models. *Mon. Weather Rev.*, 119, 1057-1074.

Jakob, C., 1994: The Impact of the New Cloud Scheme on ECMWF's Integrated Forecast System (IFS). Proceedings of ECMWF/GEWEX Workshop on Modelling, Validation and Assimilation of Clouds, ECMWF, November 1994.

Jakob, C., and Rizzi, R., 1996: Evaluation of model OLR in cloudy regions using TOVS 1b data. ECMWF Research Department Memorandum R60.1/CJ/138/PA.

Janssen P., Beljaars A., Simmons A., Viterbo P., 1992: On the determination of the surface stress in an atmospheric model. *Mon. Weather Rev.*, 120, 2977-2985.

- Jarraud M., Simmons A., Kanamitsu M., 1988: Sensitivity of medium-range weather forecasts to the use of an envelope orography. *Quart. J. Roy. Meteor. Society*, 114, 989-1025.
- Lott, F., and Miller, M. J., 1997: A new subgrid-scale orographic drag parametrization: Its formulation and testing. *Quart. J. Roy. Meteor. Society*, 123, 101-127.
- Louis J.-F., 1979: A parametric model of vertical eddy fluxes in the atmosphere. *Boundary-layer Meteorological*, 17, 187-202.
- Mahfouf, J.F., 1991: Analysis of soil moisture from near surface parameters: A feasibility study. *J. Appl. Meteor.*, 30, 1534-1547.
- Miller M., Beljaars A., Palmer T., 1992: The sensitivity of the ECMWF model to the parametrization of evaporation from the tropical oceans. *J. Climate*, 5, 418-434.
- Miller M., Palmer T., Swinbank R., 1989: Orographic gravity - wave drag: its parametrization and influence in general circulation and numerical weather prediction model. *Meteor. Atmos. Phys.*, 40, 84-109.
- Morcrette J.-J., 1991: Radiation and cloud radiative properties in the European Centre For Medium-Range Weather Forecasts forecasting system. *J. Geoph. Res.*, 96, 9121-9132.
- Morcrette J.-J., 1990: Impact of changes to the radiative transfer parametrization plus cloud optical properties in the ECMWF model. *Mon. Weather Rev.*, 118, 847-873.
- Ritchie H., Temperton C., Simmons A.J., Hortal M., Davies T., Dent D., Hamrud M., 1995: Implementation of the Semi-Lagrangian Method in a High Resolution Version of the ECMWF Forecast Model. *Mon. Weather Rev.*, 123, 489-514.
- Simmons A.J., Burridge D.M., Jarraud M., Girard C., Wergen W., 1989: The ECMWF medium-range prediction models. Development of the numerical formulations and the impact of increased resolution. *Meteorol. Atmos. Phys.*, 40, 28-60.
- Simmons A.J., Dent D., 1989: The ECMWF multi-tasking weather prediction model. *Computer Physics Reports*, 11, 165-194.
- Slingo J.J., 1987: The development and verification of a cloud prediction scheme for the ECMWF model. *Q. J. R. Meteorol. Soc.*, 213, 899-927.
- Tiedtke M., 1984: The effect of penetrative cumulus convection on the large scale flow in the general circulation model. *Beitr. Physics Atmos.*, 57, 216-239.

- Tiedtke M., 1989: A comprehensive massflux scheme for cumulus parametrization in large-scale models. Mon. Weather Rev., 117, 1779-1800.
- Tiedtke M, 1993: Representation of clouds in large-scale models. Mon. Weather Rev., 121, 3040-3061
- Viterbo, P., and Beljaars, A.C.M., 1995: An improved land surface parametrization scheme in the ECMWF model and its validation. J. Clim., 8, 2716-2748.
- Viterbo, P., and Courtier, P., 1995: The importance of soil water for medium-range weather forecasting. Implications for data assimilation. International workshop of slowly varying components of predictable atmospheric motions, Beijing, China, 7-10 March 1995. PWPR Rep. Ser. No. 6, WMO/TD No. 652, 121-130.
- Viterbo, P., 1996: The representation of surface processes in general circulation models. Doctorial thesis, ECMWF, 1-201.
- Wallace J. M, Tibaldi S.,and Simmons A. J., 1983: Reduction of systematic forecast errors in the ECMWF model through the introduction of an envelope orography. Q. J. R. Meteorol. Soc., 109, 683-717.

### ***References relating to ECMWF Re-Analysis Validation Partners***

- Arpe, K., 1994: Estimation of Global Precipitation Using the ECMWF Analysis-Forecasting Scheme - Remote Sensing Rev., Vol. II, 93-105.
- Edwards, J. M. and Slingo, A., 1996: Studies With a Flexible New Radiation Code, I: Choosing a Configuration for a Large-scale Model - Q. J. R. Meteorol. Soc., 122, 698-719.
- Slingo, A. and Webb, M. J., 1992: Simulation of clear-sky outgoing longwave radiation over the ocean using parameter simulation - Q. J. R. Meteorol. Soc., 118, 1117-1144.

